

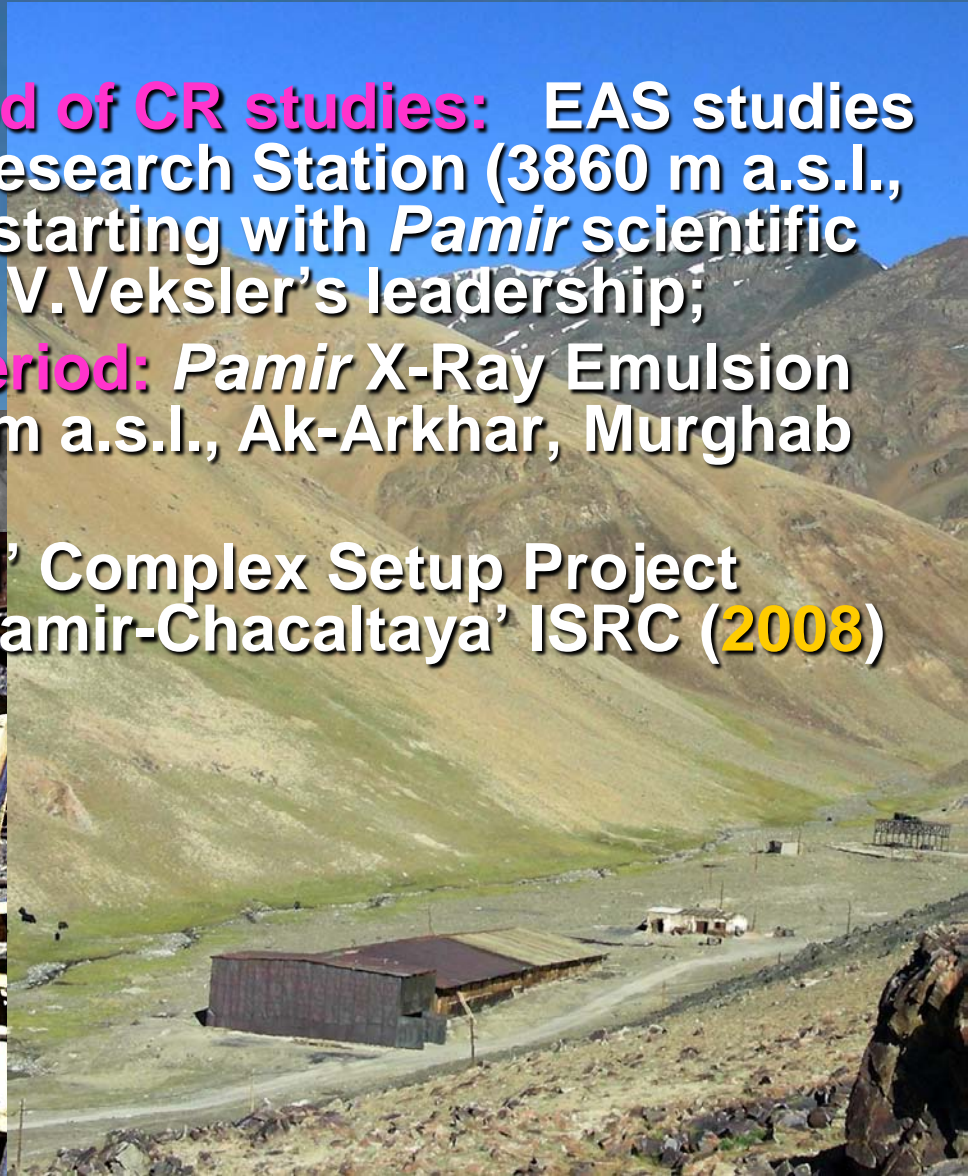
Cosmic Ray studies at the Pamirs: the Past, the Present and the Future

*(The Third Turn of CR Studies at
the Pamirs)*

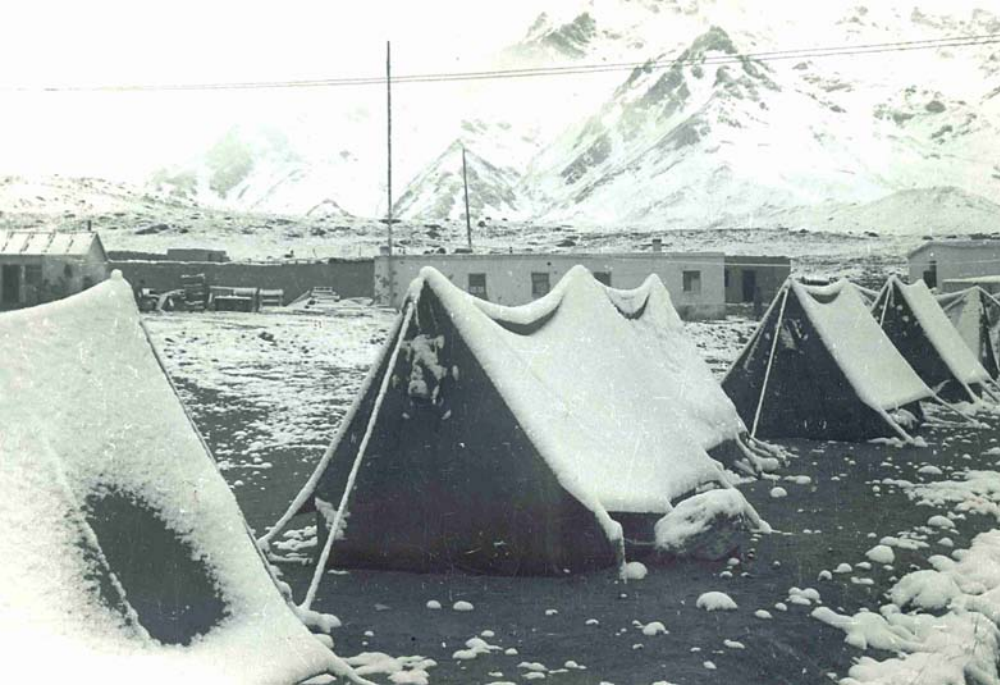
CR Conference, Tbilisi, 06-07 December 2012

Historical and Scientific Background of Cosmic Ray Researches at the Pamirs

- **1947 – 1961** - **'Heroic' period of CR studies:** EAS studies at the *Pamir* High-Altitude Research Station (3860 m a.s.l., Chechky, Murghab region) starting with *Pamir* scientific expeditions (**1944-46**) under V.Veksler's leadership;
- **1971 – 1994** - **'Romantic' period:** *Pamir* X-Ray Emulsion Chamber Experiment (4370 m a.s.l., Ak-Arkhar, Murghab region);
- **2012 – 2xxx** – the 'Pamir-XXI' Complex Setup Project after establishment of the 'Pamir-Chacaltaya' ISRC (**2008**)



'Heroic' period of CR studies (1947 – 1961)

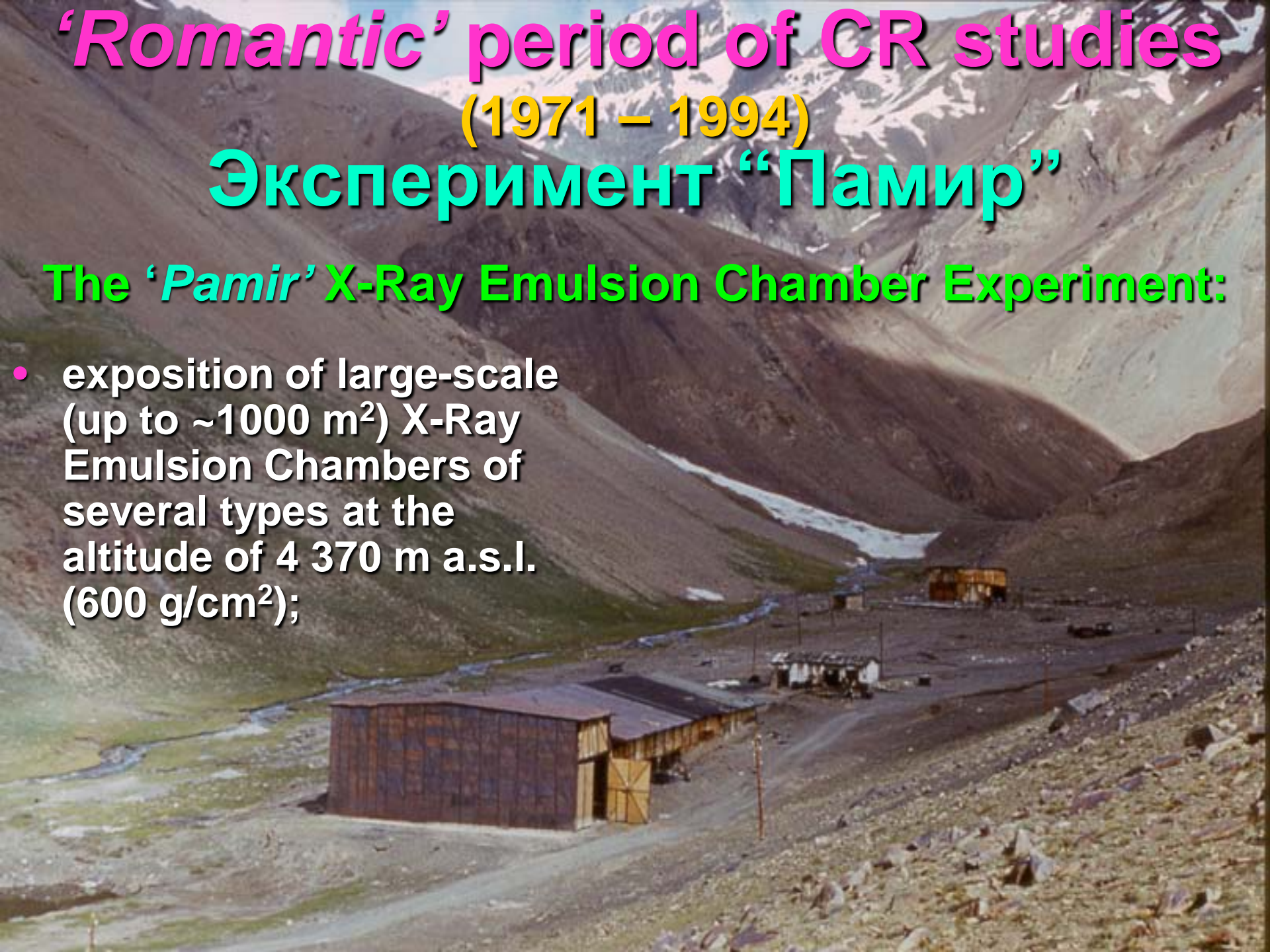


'Romantic' period of CR studies **(1971 – 1994)**

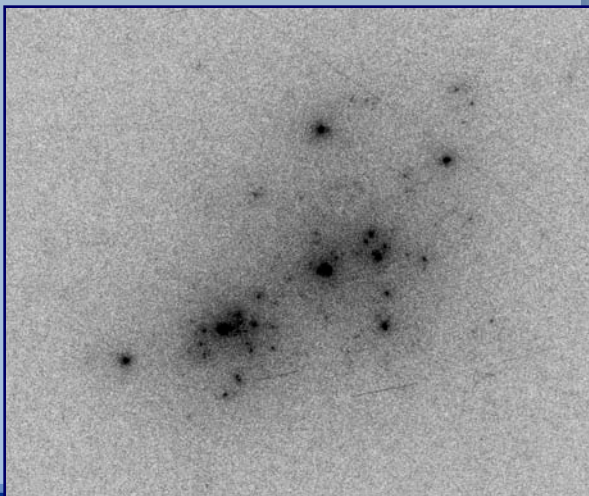
Эксперимент "Памир"

The 'Pamir' X-Ray Emulsion Chamber Experiment:

- exposition of large-scale (up to $\sim 1000 \text{ m}^2$) X-Ray Emulsion Chambers of several types at the altitude of 4 370 m a.s.l. (600 g/cm^2);



The 'Pamir' experiment



Observables:

$n_{\gamma,h}$, $E_{\gamma,h}$, $\Sigma E_{\gamma,h}$,
 x , y , $R_{\gamma,h}$
 and various combinations

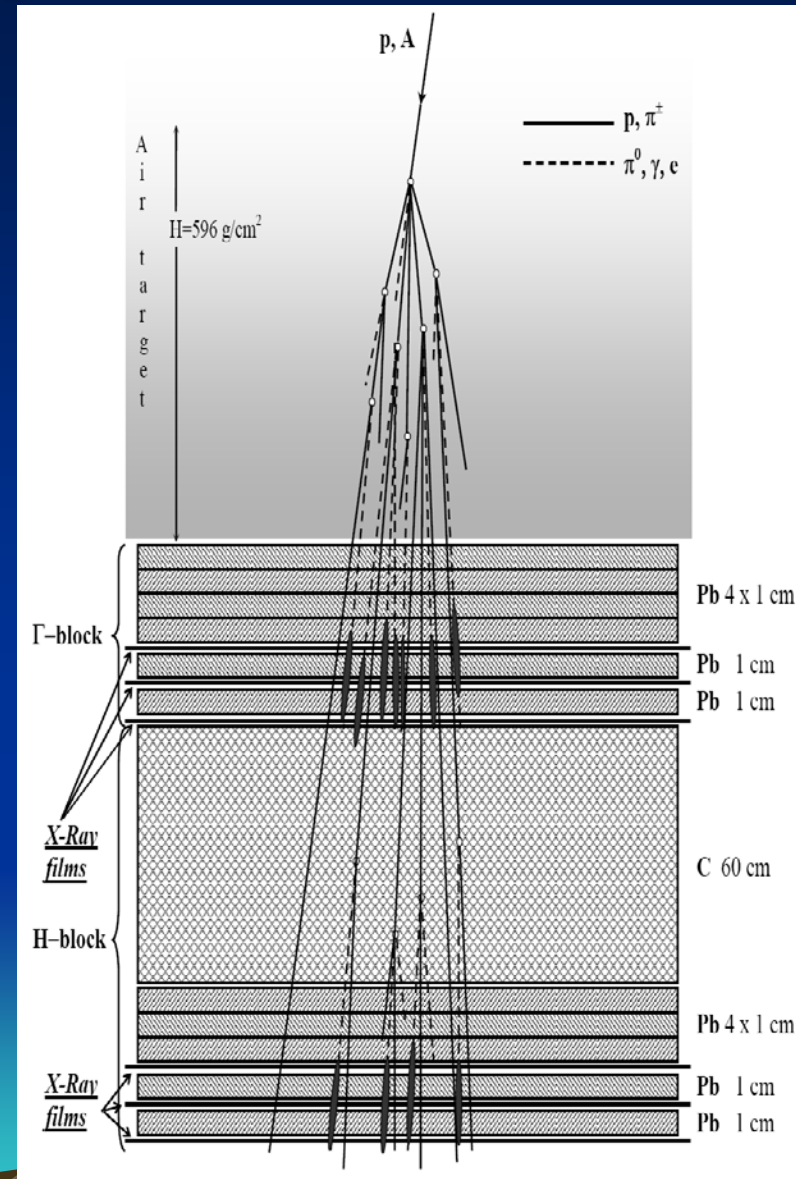
A family definition and selection criteria:

a collimated ($\Delta\theta \leq 3^\circ$, $\Delta\varphi \leq 15^\circ$) bundle of particles originated from one PCR particle

$\Sigma E_\gamma \geq 100$ TeV, $n_\gamma \geq 3$, $E_\gamma \geq E_{th} = 4$ TeV, $E_h^{(\gamma)} \geq E_{th}$, $R_{\gamma,h} \leq 15$ cm

Total exposition $ST \sim 4000$ m²•yr

Available statistics: $N_f \approx 2000$



The Pamir-Chacaltaya experimental results

Since 1980, the members of the *Pamir* collaboration worked side by side with physicists engaged in the *Mt.Chacaltaya Experiment* in the framework of the *Pamir-Chacaltaya Joint EC Experiment* and carried out several joint expositions both at the Pamirs and Mt.Chacaltaya the results of which were analyzed in numerous joint papers:

- In the energy range $E_0 = 5 \cdot 10^{14} - 3 \cdot 10^{15}$ eV which corresponds to released energies $\Sigma E_\gamma = 100 \div 400$ TeV, QGS model-inspired simulation codes (MC0, MQ, etc.) incorporating hard jet production and based on extrapolation of accelerator data produce a good fit to the main experimental results;
- estimation of the inelastic cross-section for $p^{14}N$ interactions gave a value of 360 ± 40 mb;
- increase of the inelasticity coefficient K for $p^{14}N$ reactions from $K=0.5$ at accelerator energies up to $K=0.78$ at $E_0 \sim 10^{16}$ eV;

The Pamir-Chacaltaya experimental results

- scaling violation in the fragmentation region for pion production was established, i.e., the inclusive cross-section falls 2-3 times at $x = 0.3$, when the energy increases from that attainable with accelerators, due to re-scattering of particles from nucleons inside a nucleus;
- estimation of transversal cross-section for quark-gluon string production $\sigma_{\text{jet}} = (24 \pm 7) \text{ mb}$ at jet transverse momentum $p_{\text{t}}^{\text{jet}} \geq 3 \text{ GeV}/c$ and $X_{\text{j}}^{\text{F}} > 0.05$;
- existence of the Landau-Pomeranchuk-Migdal effect was confirmed.

Still, even in the low energy range $E_0 = 5 \cdot 10^{14} - 3 \cdot 10^{15} \text{ eV}$ experimental data exhibit larger fluctuations than simulated ones which can be account for by under estimation of chamber response only partially (Centauro events, penetrating particles, etc).

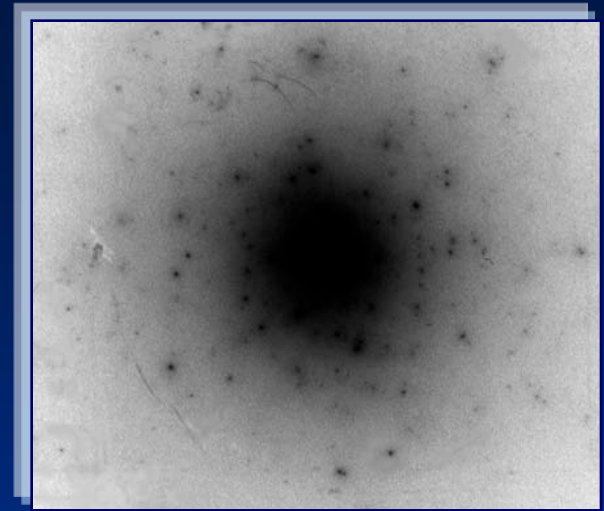
Unusual events

In the energy range $4 \cdot 10^{15} - 10^{17}$ eV significant discrepancies between experimental and simulated data are observed. The most challenging phenomena are:

- a high intensity of multi-core *halo* events;
- the coplanar emission of the most energetic hadrons and γ -rays in the multiple particle production;
- Centauro events with abnormal ratio of charged to neutral particles;
- abnormal behavior of a hadron absorption curve, which significantly deviates from exponential law at large depth in lead absorber.

Halo events

If $E_0 \geq 10^{16}$ eV, a sufficiently high number of overlapping under-threshold EPhC may overlap creating an optical “halo”, i.e., a large diffuse optical spot inside the corresponding γ -family with a visible energy $\Sigma E_\gamma \geq 500$ TeV. Sometimes area of a halo $S \sim \text{cm}^2$. The fraction of halo events increases with family energy and, at $\Sigma E_\gamma \geq 1000$ TeV, amounts up to 70 %.



Scanner image of ‘FIANIT’ halo event

$S_{D=0.5} = 1'017 \text{ mm}^2$
visible energy $E = (2\div 3) \cdot 10^{16} \text{ eV}$
(Isodence $D=0.5$ corresponds to particle density 0.04 mm^{-2})

Halo event selection criteria: $\Sigma E_\gamma \geq 500 \text{ TeV}$, $n_\gamma \geq 3$, $E_\gamma \geq 4 \text{ TeV}$,
 $S_{D=0.5} \geq 4 \text{ mm}^2$ or $\Sigma S_{D=0.5}^i \geq 4 \text{ mm}^2$, $S_{D=0.5}^i \geq 1 \text{ mm}^2$ $R_\gamma \leq 15 \text{ cm}$

Statistics: $N_H = 61$, $ST = 3000 \text{ m}^2 \cdot \text{year}$

$$N_f^{\text{tot}} (\Sigma E_\gamma \geq 500 \text{ TeV}) = 143$$

Simulation of Halo events

MC0 is a QGS-model which:

- satisfactory reproduces the main characteristics of γ -families with $\Sigma E_{\gamma} = 100\div 400$ TeV;
- describe well the halo size spectrum of γ -families with $\Sigma E_{\gamma} \geq 500$ TeV

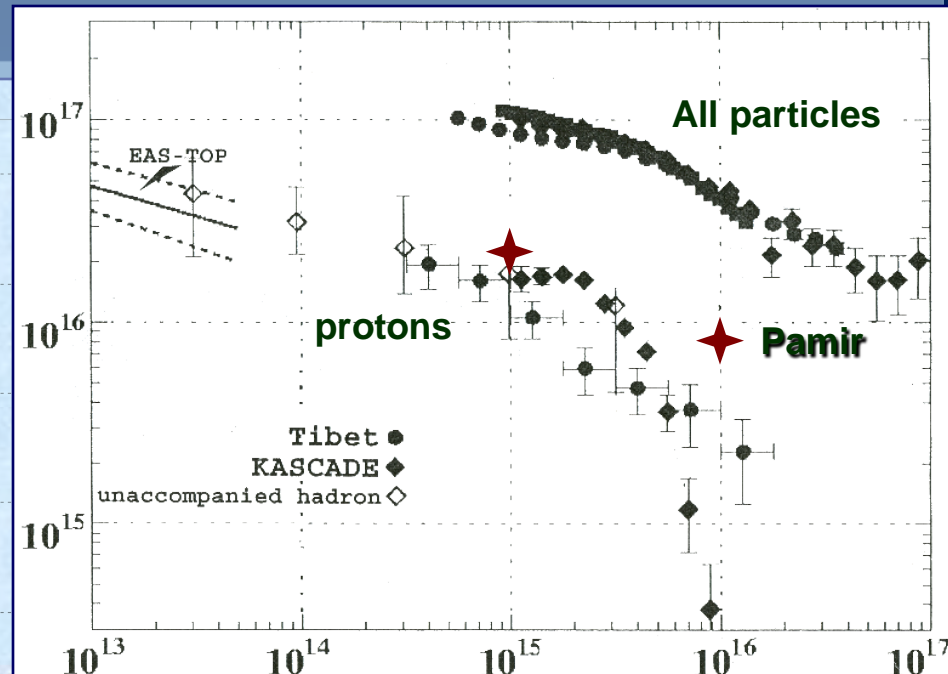
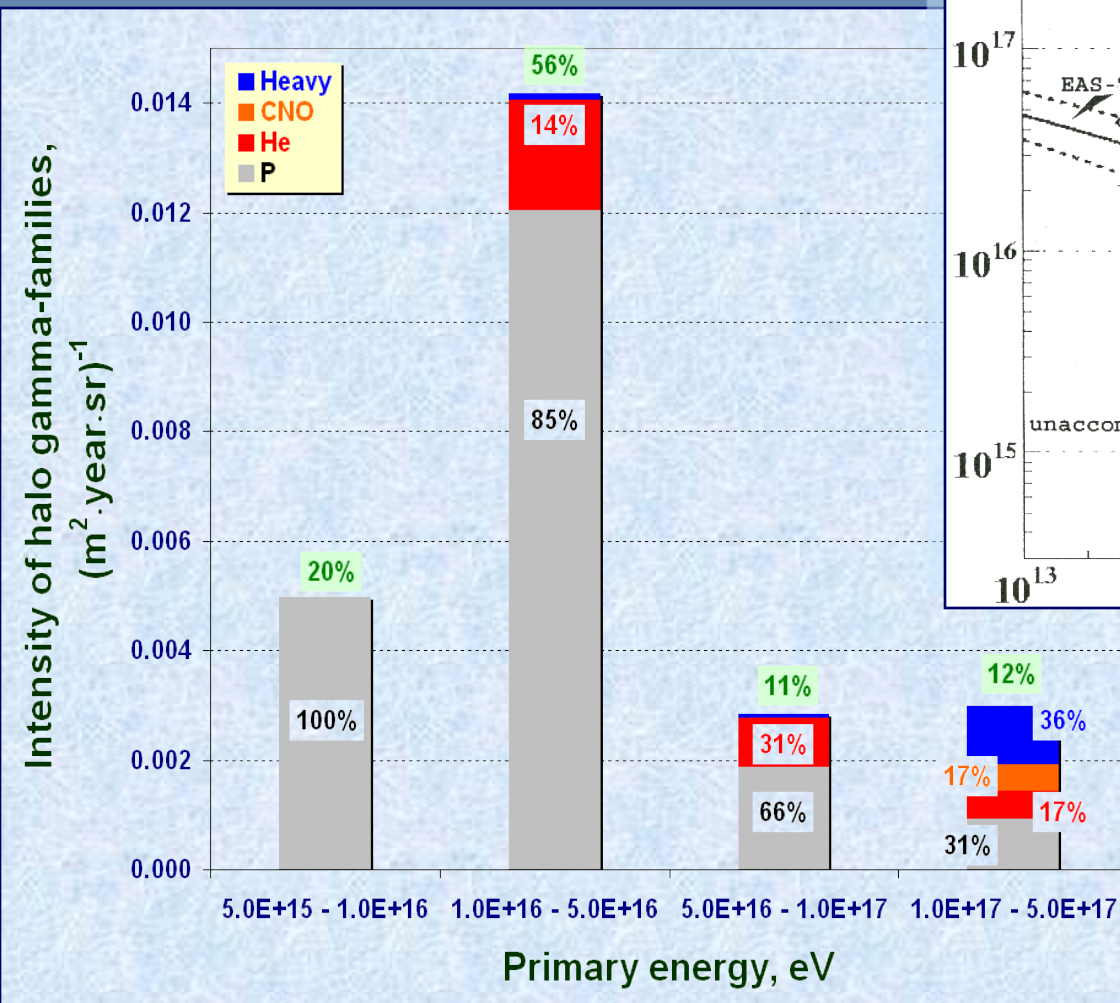
Assumed PCR mass composition:

Energy, eV		10^{14}	10^{15}	10^{16}	10^{17}
Primary particle fraction, %	<i>P</i>	36	33	27	20
	<i>α</i>	20	20	18	14
	<i>A > 4</i>	44	47	55	66

Simulation of Halo events

Contribution of primary particles from different energy intervals to intensity of halo gamma-families

Energy spectra of protons according KASCADE and Tibet data



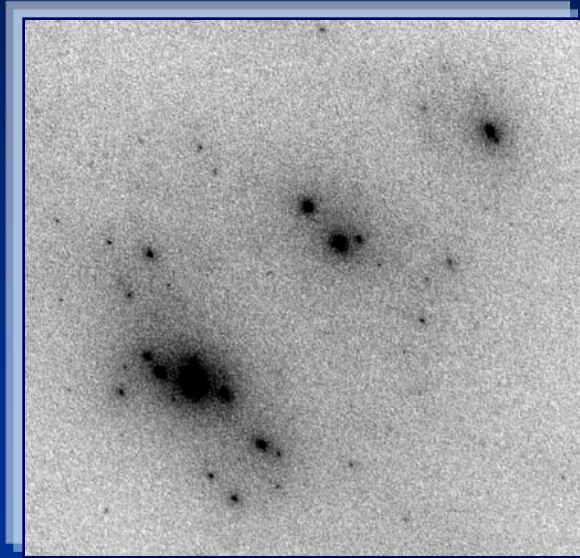
Fraction of halo γ -families with $\Sigma E_\gamma \geq 500$ TeV produced by different PCR nuclei:

P	He	A > 4
80%	10%	10%

Conclusions based on halo γ -family intensities

- Proton fraction in the PCR mass composition at $E_0 \geq 10^{16}$ eV is not less than 15%.
- The results of the *Pamir* experiment contradict to claims for drastic vanishing of protons and α -particles at energies around 10^{16} eV.
- Significant increasing of proton fraction in the PCR at energies $\geq 10^{17}$ eV is not enough to agree experimental data with the simulations.

Phenomenon of coplanar emission of hadrons



An example of aligned
3-core *halo* event

The effect, first observed in the *Pamir* experiment, manifested itself as a strong tendency for tracks of the most energetic particles in γ -h families as well for their narrow bundles (family cores) to be aligned along a certain straight line in the target plane .

The highest energetic cores (HEC) in a family can be represented by:

- halo cores;
- γ -clusters or reconstructed π^0 ;
- single gamma-ray or hadron.

For quantitative definition of events with N cores aligned along one straight line, the following criterion was introduced:

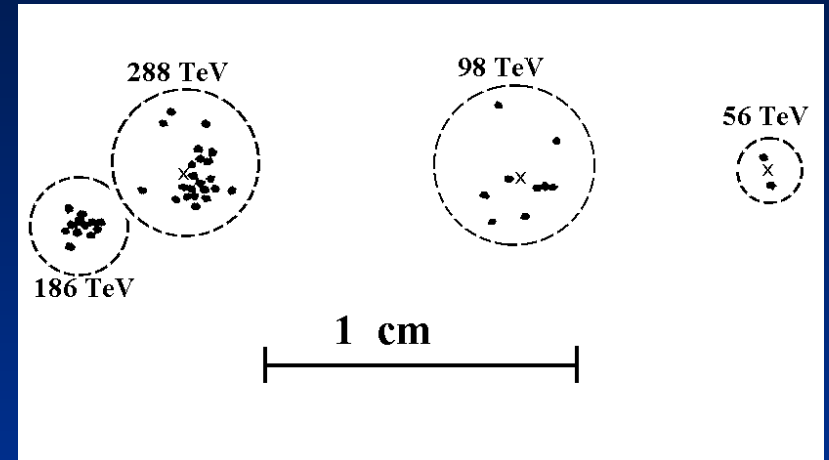
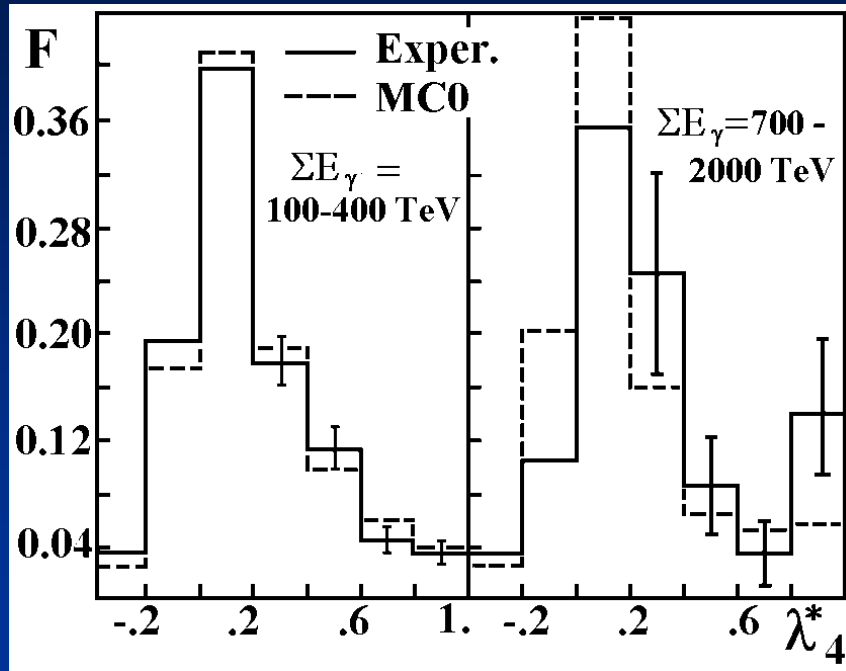
$$\lambda_N = \frac{\sum_{i \neq j \neq k}^N \cos 2\varphi_{ij}^k}{N(N-1)(N-2)}$$

where φ_{ijk} is the angle between the straight lines connecting the i -th and j -th cores with the k -th core.

The parameter $\lambda_N = 1$ in the case of complete alignment of N cores along one straight line and tends to $-1/(N-1)$ in an isotropic distribution case.

Families containing N -core structures, composed of the HEC and characterized by $\lambda_N \geq \lambda_C = 0.8$ are referred to as aligned events.

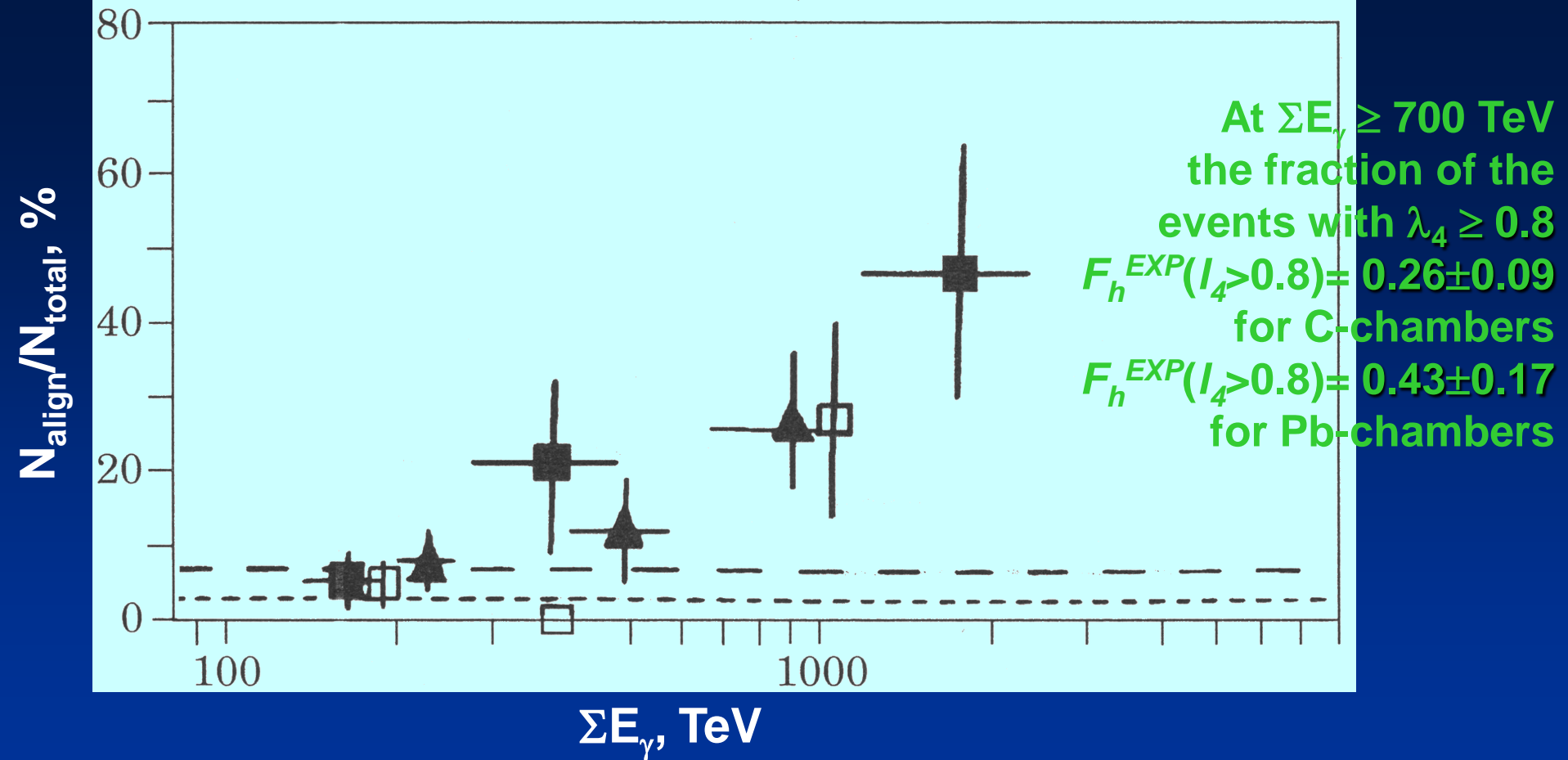
Aligned γ -families



Example of the target diagram of an aligned superfamily. Circles schematically show particles unified into clusters.

λ_4 -distribution of experimental and simulated γ -families in two energy ranges after applying of clusterization procedure

$$\chi_{ij} = R_{ij} \sqrt{E_i E_j} \leq \chi_c = 48 \text{ TeV} \cdot \text{cm}$$



Dependence of the fraction of families with alignment on ΣE_γ

Experiment: ■ Pb-chamber data, □ C-chamber of the Pamir Joint Experiment, ▲ Pamir C-chamber

Simulations: ——— simulated families with MC0-model randomly incident objects
- - - simulated families with MC0-model randomly incident objects

Main treats of coplanar production of hadrons in the most forward region:

- *existence of an energy threshold for aligned event production ($\Sigma E_\gamma \geq 700 \text{ TeV} \leftrightarrow E_0 \geq (5\div 8) \cdot 10^{15} \text{ eV}$);*
- *related to most energetic particles;*
- *large transverse momentum (about several GeV/c);*
- *A ratio of longitudinal component $\langle p_t \rangle^{\parallel}$ of the average transverse momentum of secondaries to transverse component $\langle p_t \rangle^{\perp}$, determined in reference to the coplanarity plane, can be estimated as $\langle p_t \rangle^{\parallel} / \langle p_t \rangle^{\perp} \approx \langle R_c \rangle_4^{\parallel} / \langle R_c \rangle_4^{\perp} = 12 \pm 3$;*
- *considerable cross-section for the production ($\sigma_{\text{copl}}^p \sim \sigma_{\text{inel}}^p$).*

Aligned events in Stratosphere

Two superfamilies induced by the PCR particles with $E_0 \geq 8 \cdot 10^{15}$ eV were once detected at the balloon and aircraft-borne EC experiments by chance and both of them appeared to be extremely aligned:

Event	H (g/cm ²)	E _{th} /TeV/	N _γ	N _h	ΣE _γ /TeV/	ΣE _h /TeV/	λ ₄	λ ₃₈
JF2af2 (Concorde)	100	0.2	211		1586		0,998	0,95
Strana (baloon)	10	2.0	76	30	1400	2500	0,99	0,99

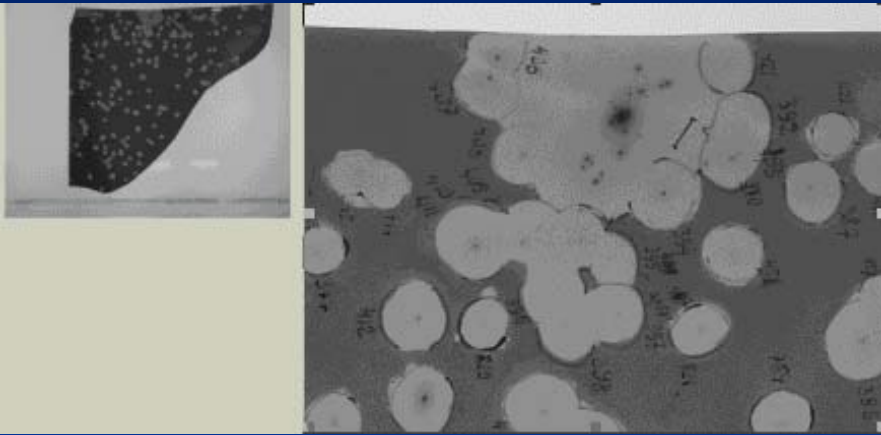
Aligned events in Stratosphere

Estimation of production heights H^{prod} above the chamber by various methods (triangulation, invariant mass distributions, etc.):

Event	H (m)	N_γ	N_h	ΣE_γ /TeV/	ΣE_h /TeV/	$\langle p_t \rangle$ GeV/c	ST /m ² •h/
JF2af2 (Concorde)	60-100	211		1586		> 10	0.06 x 400
Strana (balloon)	200- 1500	76	31	1400	2500	> 2.5	

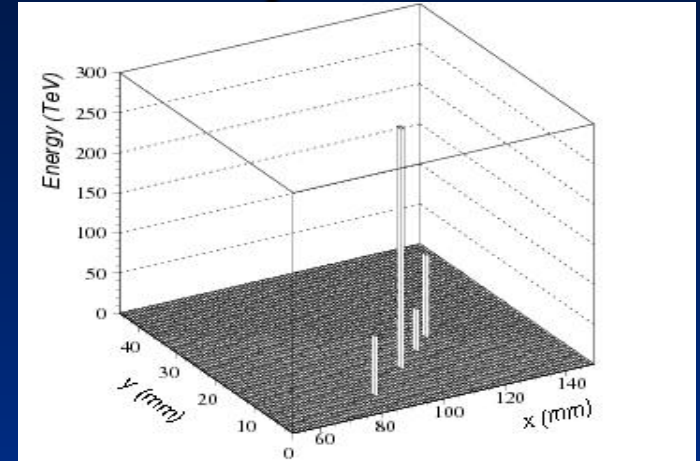
'Strana' event

Balloon-borne experiment carried out by Prof. Dobrotin and his colleagues of Lebedev Physical Institute in 1975



Estimated primary energy
 $E_0 \approx 2 \cdot 10^{16} \text{ eV}$

JF2af2 (Concorde)



- Xray film under 8 c.u.

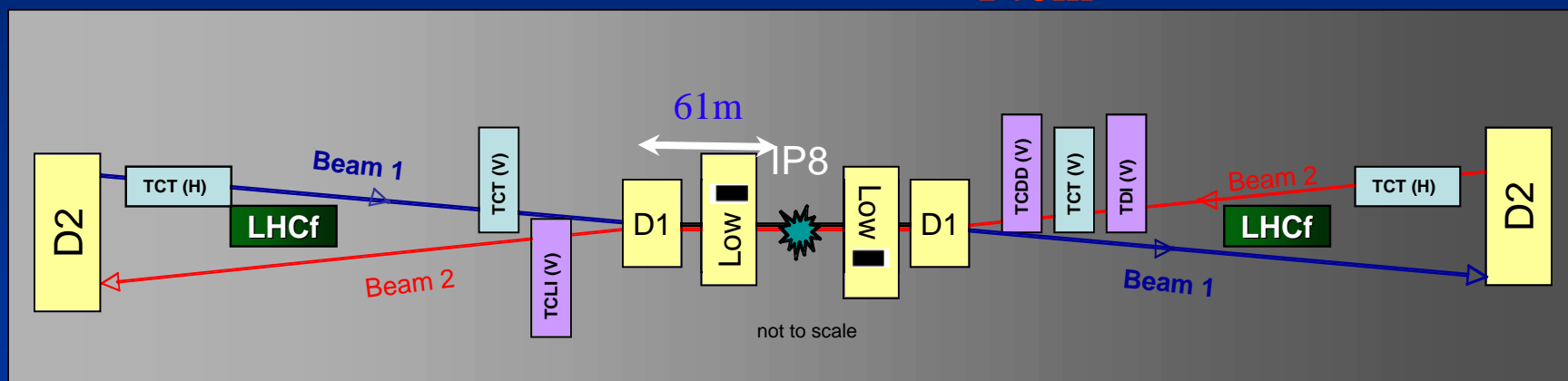
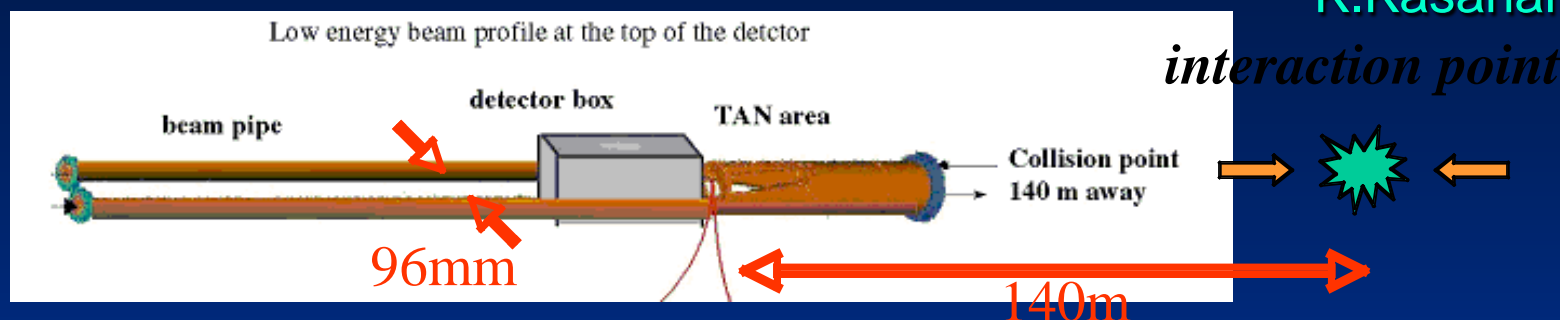
- Lego plot with the 4 most energetic Gamma 's

34 g 's are aligned (about 50% of the visible energy)
3 most energetic clusters (A,AP,B) each containing the highest energy gammas (about 33% of the visible energy) are aligned :

	A	Ap	B
$\Sigma E_{\gamma}/\text{TeV}$	331.0	455.4	610.6
N_{γ}	60	10	77
$\langle R \rangle$	8.62	0.49	10.26

Study of coplanarity by LHCf

K.Kasahara 2006

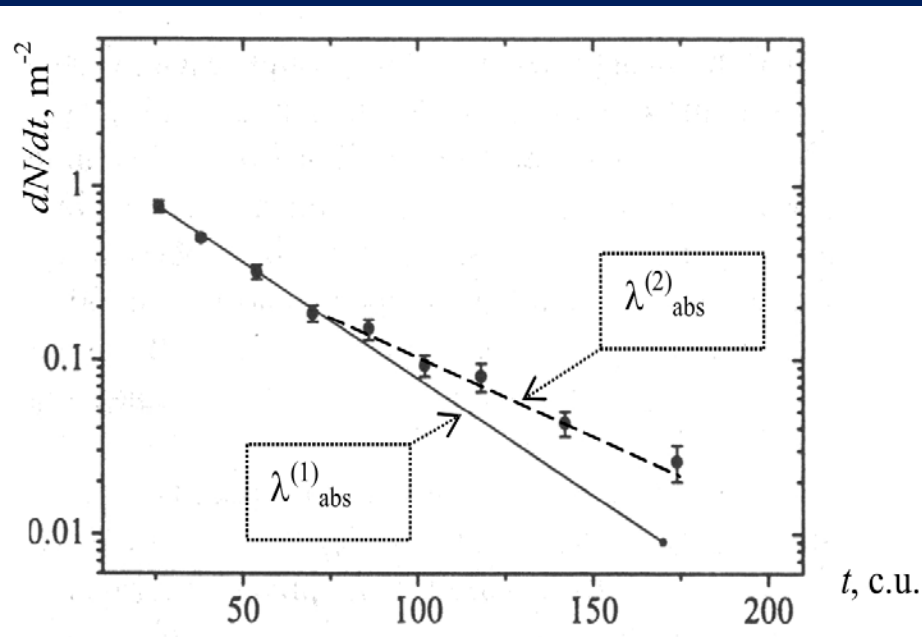


beam pipe radius ~ cm, typical Xing angle ~ 140 micro rad

Our standpoint: coplanarity effect can not be observed with LHCf detector due to its small dimensions !!!

(attainable range of $P_T^\gamma, \text{GeV}/c < 1.5 E_\gamma / 2000$)

Penetrating hadrons with abnormal absorption

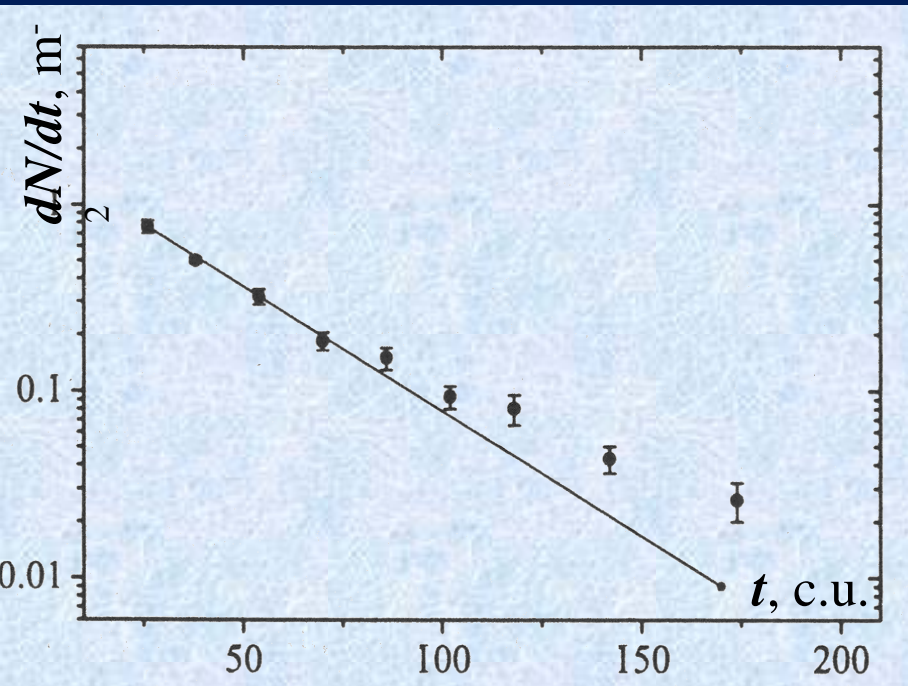


Distribution of the cascade origin points for hadrons with $E_h^{(\gamma)} \geq 6.3$ TeV obtained in the Pamir experiment by means of homogeneous Pb-chambers 110 cm thick.

In the range of 0÷70 rad. lengths, the absorption curve obeys the standard exponential law with index $\lambda_1 = (200 \pm 5) \text{ g/cm}^2$. However, at larger depths (>70 c.u.), the absorption length of hadrons in lead changes and becomes as high as $\lambda_2 = (340 \pm 80) \text{ g/cm}^2$.

This unusual phenomenon seems to be similar to that discovered earlier at the Tien Shan Mountain Station when absorption of EAS hadron cores in a hadron calorimeter was studied (a hypothesis of long-flying component of cosmic rays introduced by V.I. Yakovlev).

Penetrating hadrons with abnormal absorption



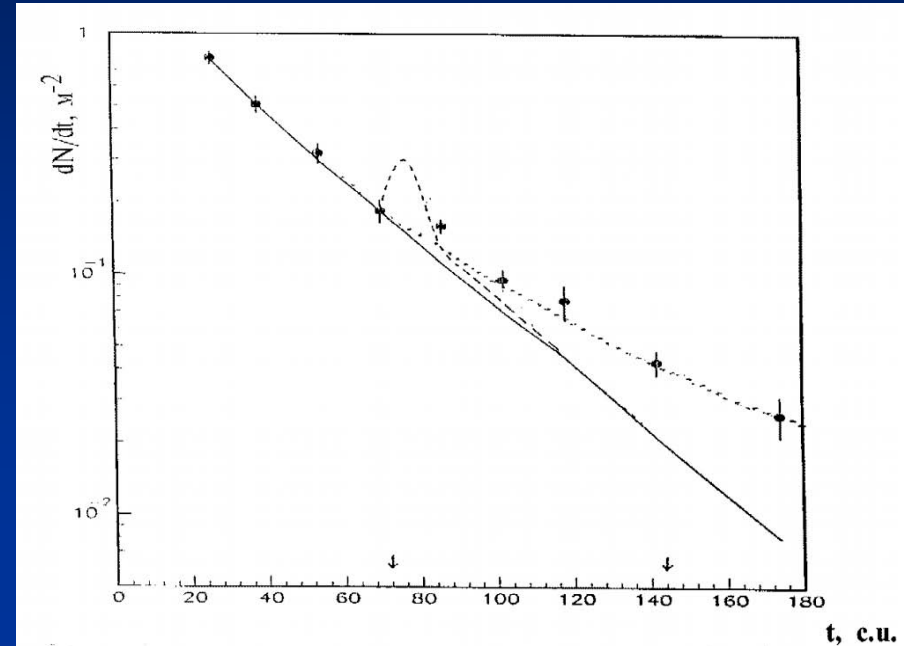
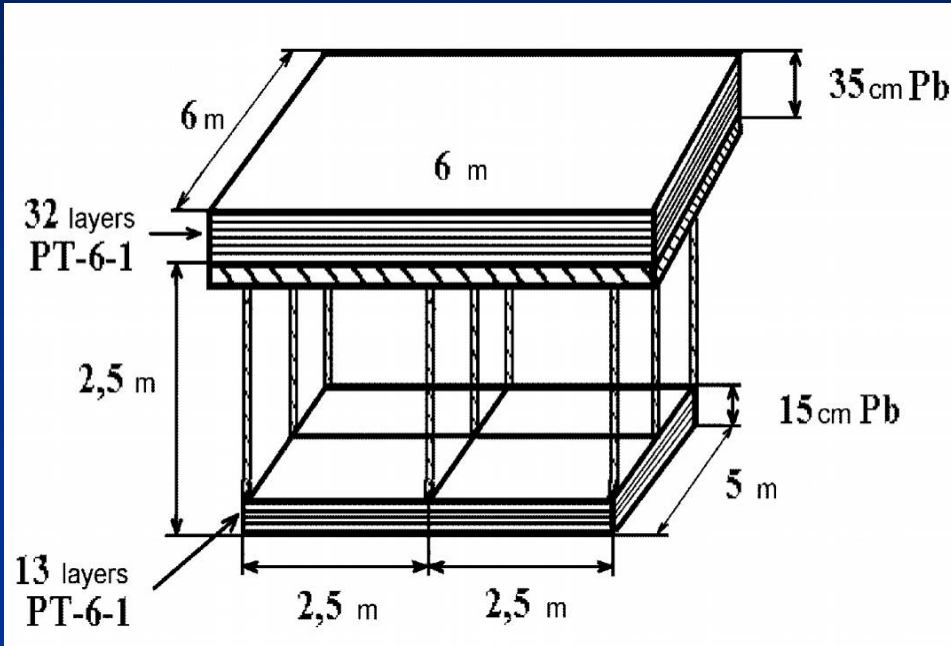
Distribution of the cascade origin points for hadrons with $E_h^{(v)} \geq 6.3$ TeV obtained in the Pamir experiment by means of homogeneous Pb-chambers 110 cm thick.

There are two possible explanations of the effect:

- considerable contribution of charm particles;
- manifestation of quark strange matter (existence of strangelets).

Testing of the charmed origin of penetrating particles

Hypothesis: Excessive cascades are initiated by charm particles
($\sigma_{\Lambda_c, D}^{\text{prod}} \approx 2 \text{ mb/nucleon}$)

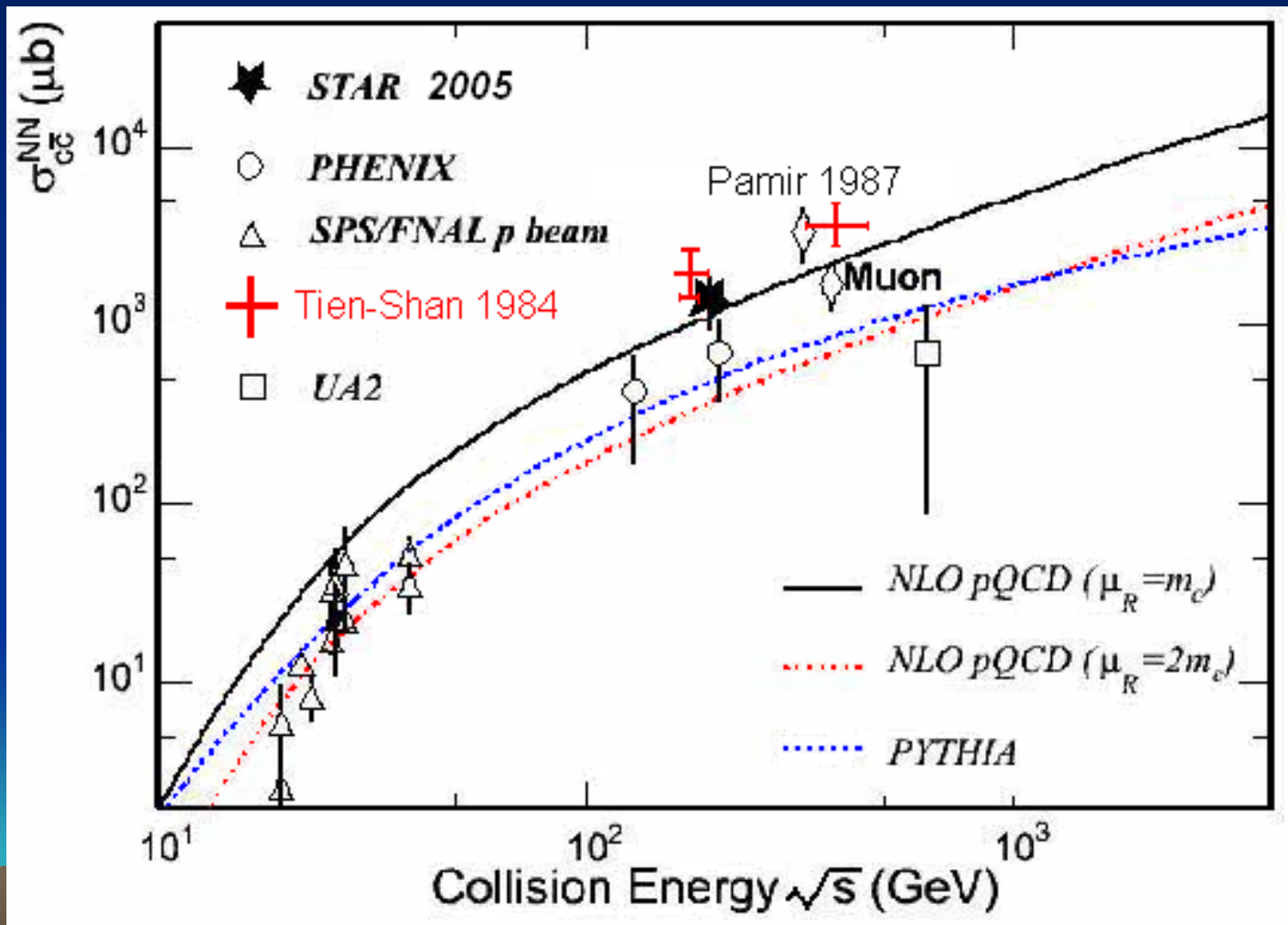


■ A Lay-out of a 2-storied XREC with 2,5 m air-gap

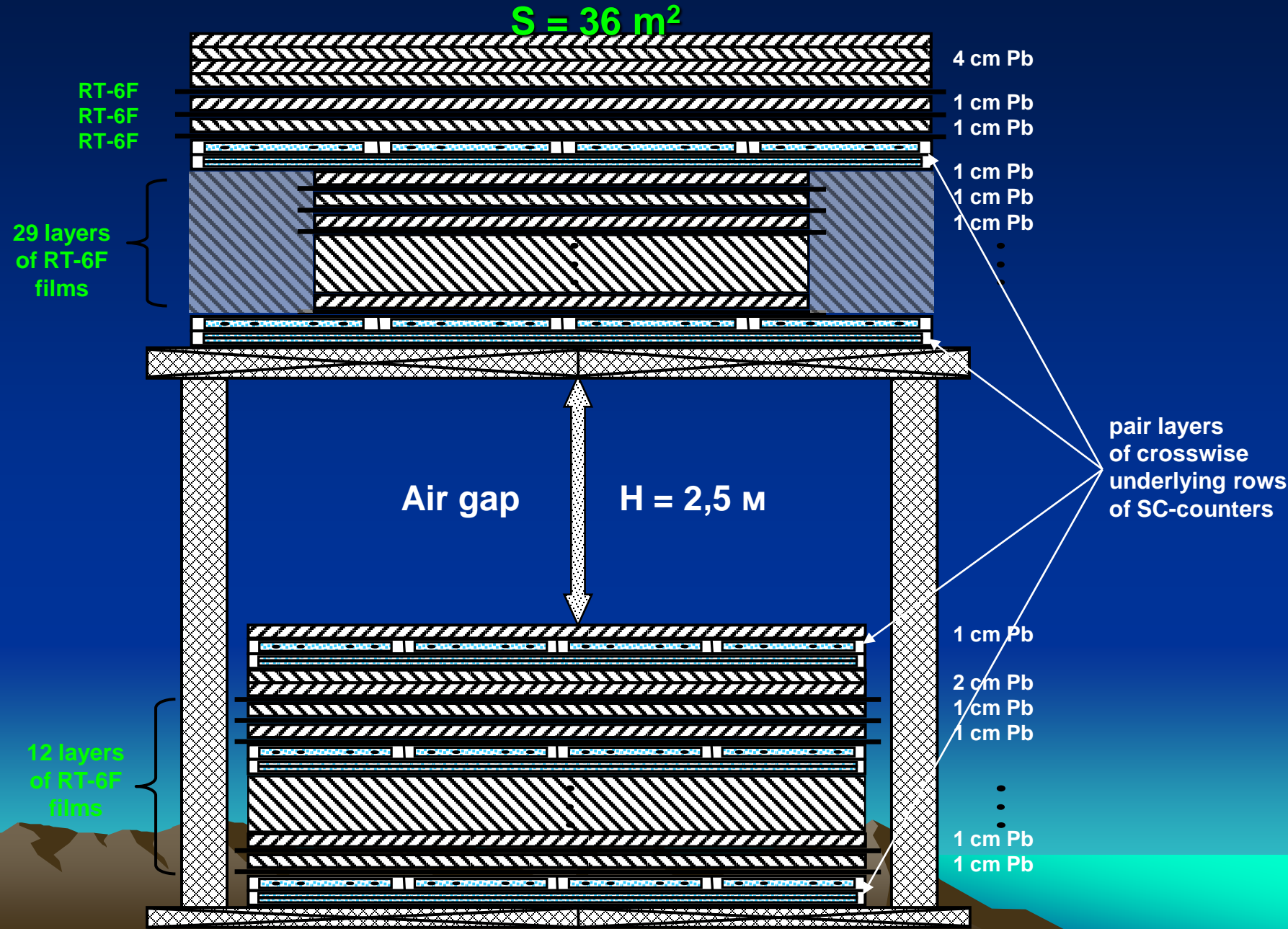
■ Distribution of cascade origin points in 2-storied XREC with 2,5 m air-gap

RHIC experiments (STAR, PHENIX)

STAR: $\sigma_{cc}^{NN} = 1,4 \pm 0,2 \pm 0,4 \text{ mb}$; PHENIX: $\sigma_{cc}^{NN} = 0,92 \pm 0,15 \pm 0,54 \text{ mb}$



Search for 'Centaurus' and strangelets at the Pamirs

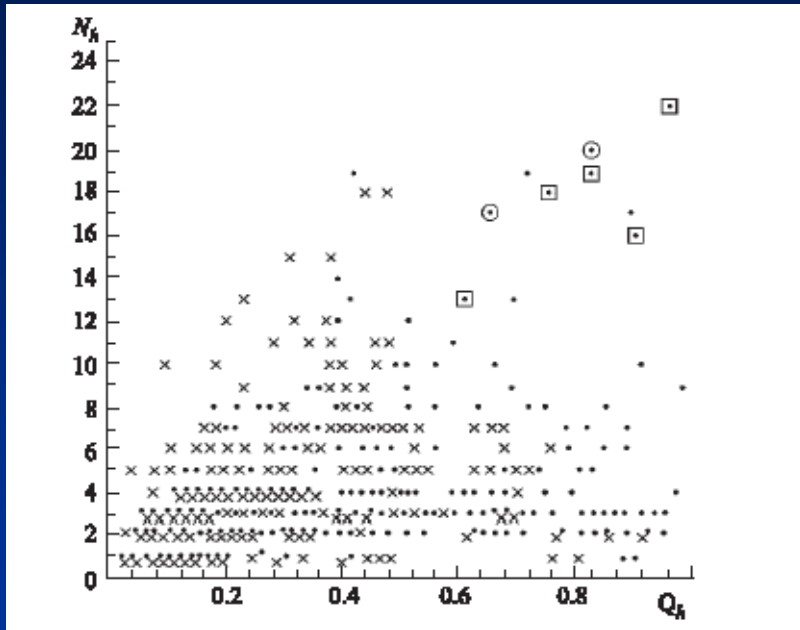


Two-storied XREC with 2.5 m air gap at the Pamirs



Tbilisi, 06-07 December 2012

Centauro-type events



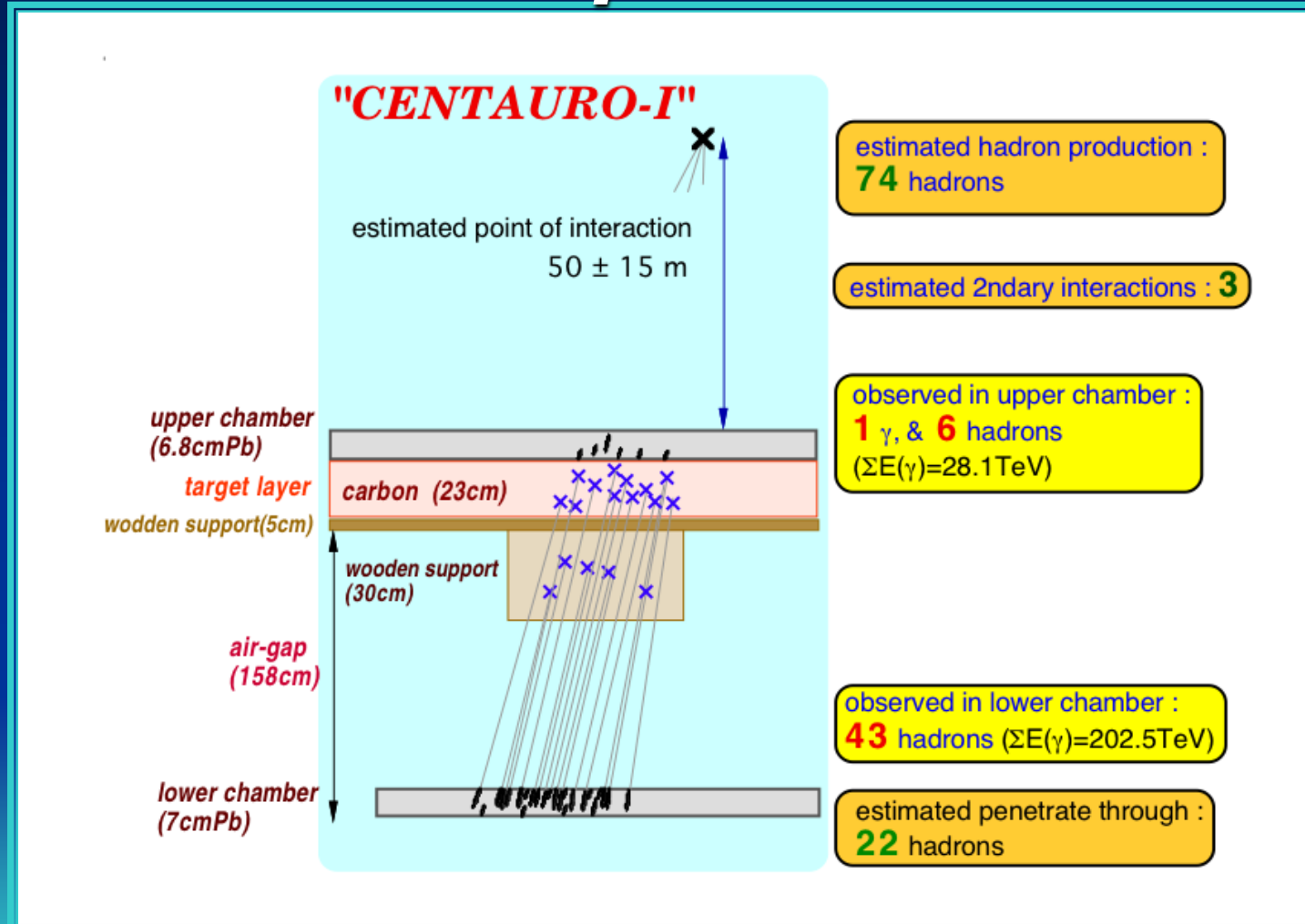
Centauro events first observed by the Japan-Brazil Collaboration in a two-storied emulsion chamber exposed at the Mt. Chacaltaya are distinguished by abnormally high fraction of energy carried by charged hadrons as compared to that of gammas.

N_h vs. $Q_h = \sum E_h^{(\gamma)} / (\sum E_\gamma + \sum E_h^{(\gamma)})$
(Dots stand for experimental events while crosses refer to simulated ones. Candidates for Centauro-type events in the *Pamir* and the *Chacaltaya* experiment data are marked by squares and circles, respectively).

The Pamir experiment:

88 γ -h families were analysed with visible energy $\sum E_\gamma + \sum E_h^{(\gamma)} \geq 100$ TeV which were detected by Pb-chambers of 60 cm thick with total exposition 132 $\text{m}^2 \cdot \text{year}$.

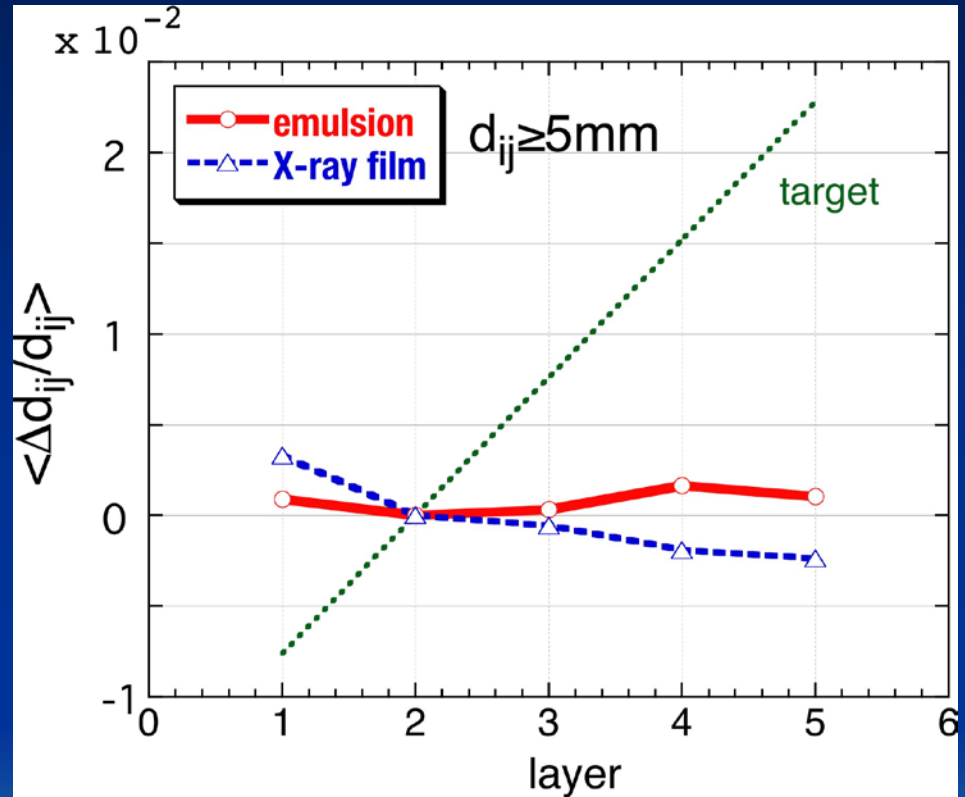
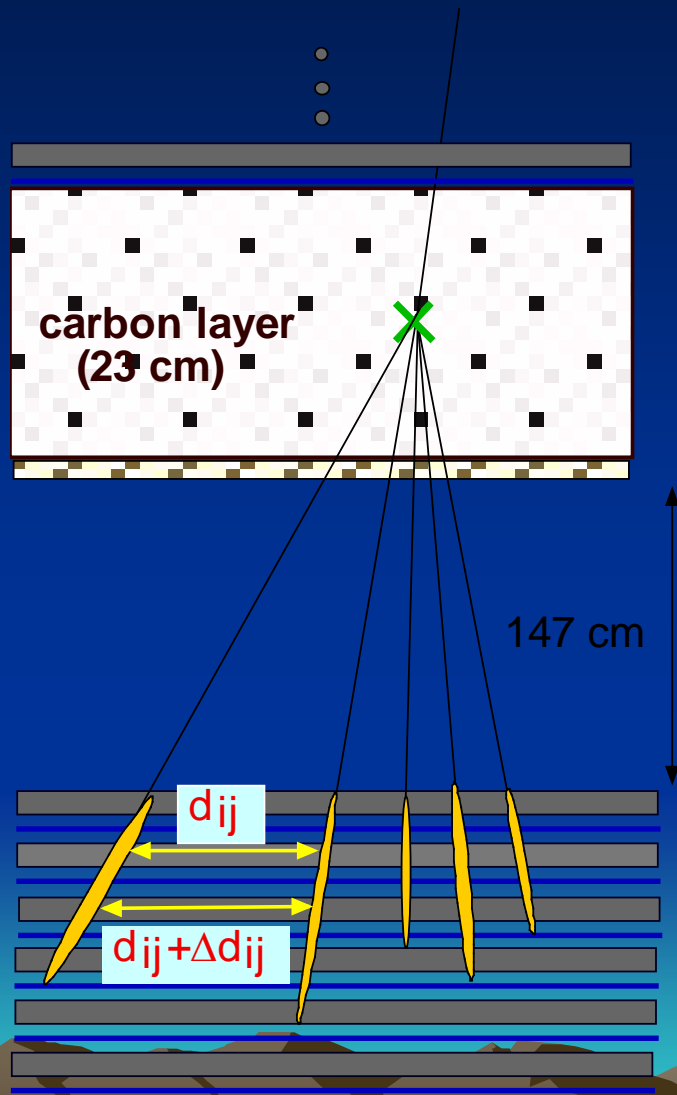
CENTAURO : original data and interpretation



$N_h \sim 100, \langle p_t \rangle \sim 1.5 \text{ GeV}/c, \text{ non-}\pi^0 \text{ production}$

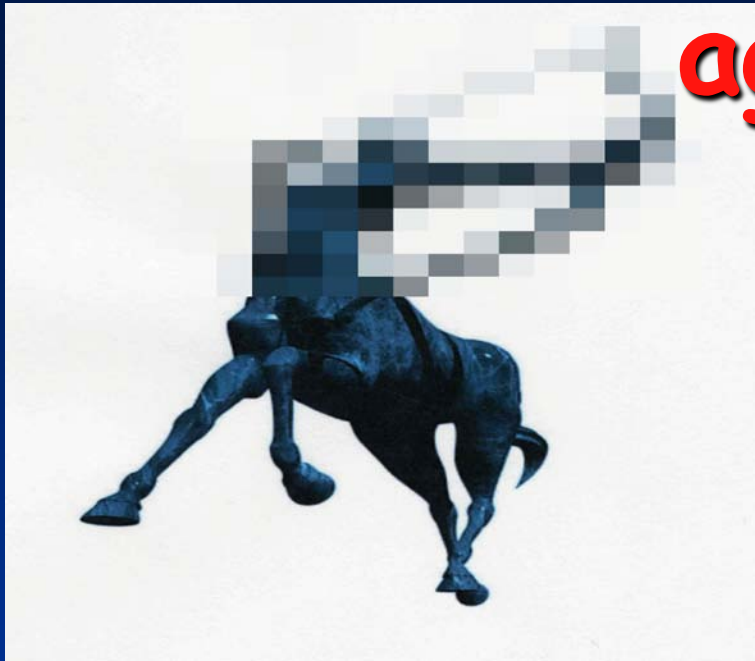
Tbilisi, 06-07 December 2012

C-jet with very large p_t and multiplicity ?



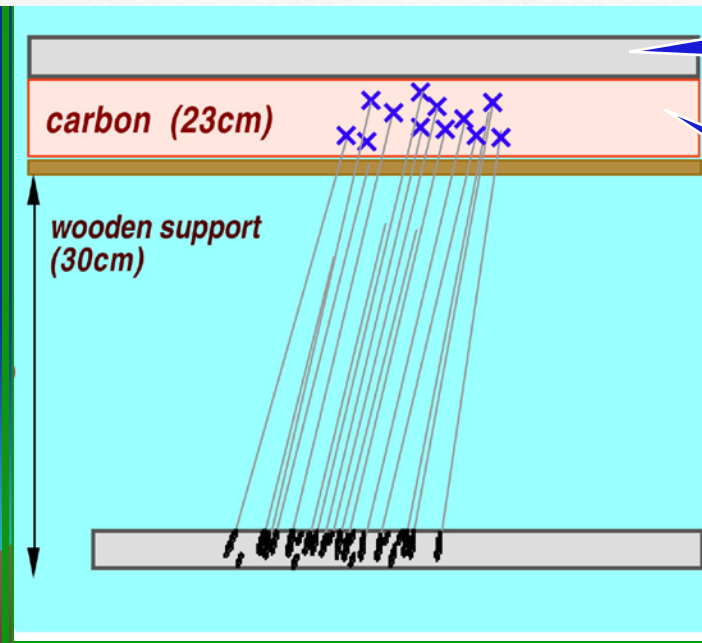
**no geometrical
convergence to target
layer !!**

again very exotic !!



*a bundle of hadrons
w/o accompanying γ -
rays*

**no collisions
in the upper chamber !!**



**≥ 28 collisions
In the target layer !!**

CONCLUSIONS

- Several new phenomena are observed in CRs with XREC at energies around and beyond the 'knee' energy which are hard to explain within SM.
- All unusual events and phenomena observed in *EC* experiments can be accounted for by an assumption of presence of highly penetrating particles in CRs which are able to penetrate deep in the atmosphere and then interact (or decay) nearby XREC producing halo events, coplanar events or Centauro-type events.

The Third Turn of CR Studies at the Pamirs

‘Pamir-XXI’

Complex Setup Project

**for Multi-Component Study of Superhigh Energy EAS and
Parental PCRs in a wide energy range around and above the “knee”**

within *‘Pamir-Chacaltaya’* ISRC

Main goals and physics problems of *'Pamir-XXI'* experiment

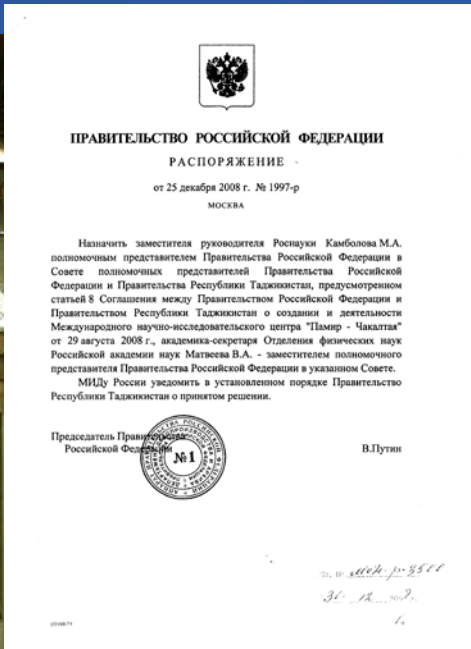
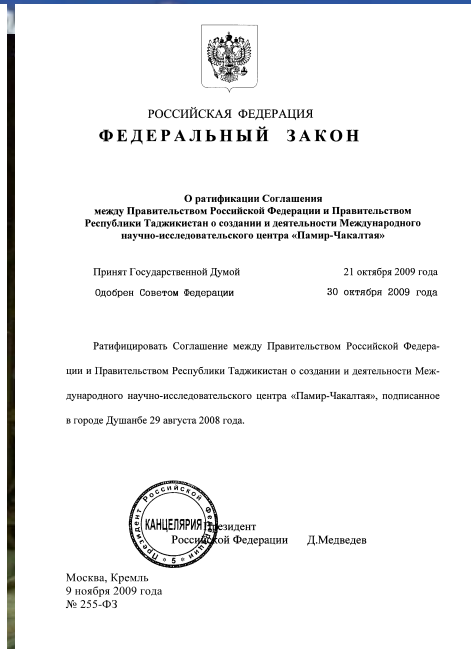
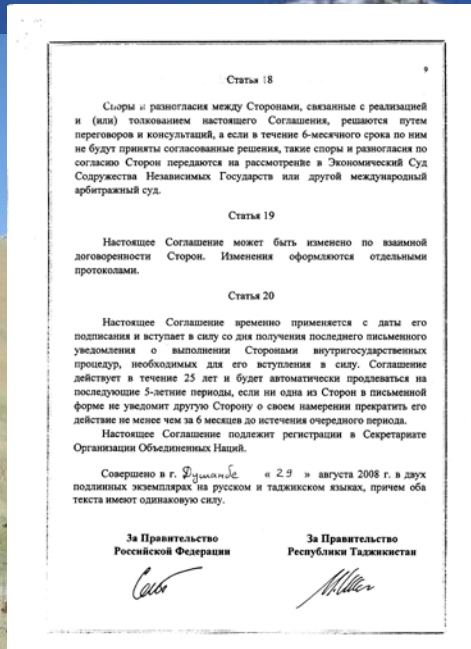
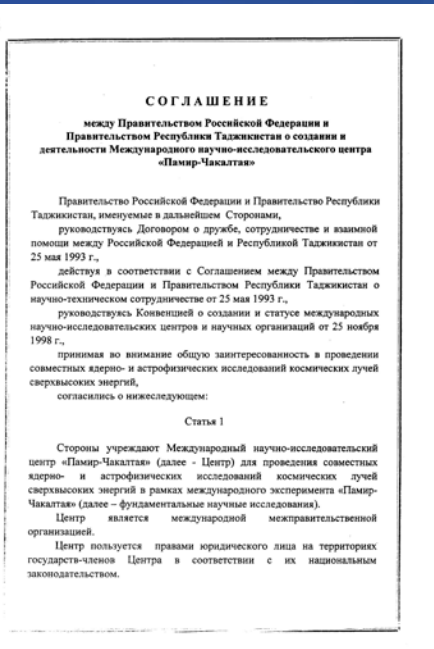
- detailed and elementwise study of the PCR energy spectra and composition by means of calorimetric methods of E_0 determination with EAS observation in a wide range of primary energies $E_0=30\div 10^6$ TeV partially overlapping that of direct observations and also containing the 'knee' at $E_0 \sim 3\div 4$ PeV and other spectrum peculiarities beyond it;
- EAS multi-component study (including muon, Čerenkov and hadronic ones as well as gamma-hadron families representing a fine structure of the EAS cores) at the depth of $H=600$ g/cm² in the atmosphere which corresponds to the maximum of EAS development at the 'knee' energy where fluctuations in the EAS development are minimal and thus accuracy of energy E_0 determination with N_e is maximal;
- simultaneous study of lateral and longitudinal EAS development, which is especially sensitive to the PCR mass composition, by means of a Čerenkov detector array and a system of Čerenkov image telescopes;

Main goals and physics problems of '*Pamir-XXI*' experiment

- a detailed study of EAS cores and their fine structure in order to clarify characteristics of hadronic interactions in a kinematic fragmentation region of an incident particle and in processes with small transverse momenta transferred ('forward physics');
- a study of diffuse gamma-rays with energies above 30 TeV and localization of Galactic γ -sources within the entire northern hemisphere of the sky with a sensitivity of $\sim 3-4\%$ I_{CRAB} for their further detailed study at setups such as CTA or AGIS;

Potential of the Eastern Pamirs

for deployment of a new large-scale astrophysical experiment



1. Foundation of the **Pamir-Chacaltaya ISRC** as an international intergovernmental organization opened for joining by any other state or scientific institution.

2. Operation of the **Ak-Arkhar experimental site** of the ISRC-PCh possessing large quantities of valuable constructional materials such as:

- rolled lead plates of 1 cm thick ($\rho=11.34 \text{ g/cm}^2$) ~ 1300 tons
- rubber plates of 3, 4, 5 cm thick ($\rho=1.24 \text{ g/cm}^2$) ~ 560 tons
- graphite blocks of 6, 10 cm thick ($\rho=1.85 \text{ g/cm}^2$) ~ 30 tons

Potential of the Eastern Pamirs

for deployment of a new large-scale astrophysical experiment

...

3. Accessibility of vast high-altitude valleys suitable for deployment of a new large-scale setup of $S \geq 1 \text{ km}^2$ in area at altitude of $H \sim 600 \text{ g/cm}^2$ corresponding to the maximum of EAS development at the 'knee' energy, where EAS size fluctuations are minimal and hence the PCR energy estimations are the most accurate.
4. Unique astroclimate of the Eastern Pamirs, characterized by a large number (~ 300) of clear (cloudless) nights a year, fairly evenly distributed over the seasons, a low content of aerosols and water vapor in the atmosphere, a weak turbulence of surface air, and besides, almost complete absence of light pollution, i.e. illumination of the night sky by artificial light sources.

Potential of the Eastern Pamirs

for deployment of a new large-scale astrophysical experiment



PROGRAM

of CR researches at the Pamirs within the *Pamir-Chacaltaya* ISRC

- Stage I, (2009-2013): assembling and exposition of **2-storied XREC**. **Physical problems**: the study of nuclear-active penetrating (long-flying) component in cosmic rays, search for and study of unusual events and phenomena beyond the Standard model such as 'centauros', 'strangelets', 'chirons', large- p_t 'halo' events, aligned (coplanar) events, etc.
- Stage II, (2012-2014): upgrading of XREC by creation of a **hybrid setup**, i.e., mounting of a burst detector under Γ -block of XREC and deployment of an air shower array of $S=80 \times 80 \text{ m}^2$ in area around the XREC, for detailed study of EAS cores.
- Stage III, perspective (2014-2020): creation of the *Pamir-XXI* **complex setup** (XREC+EAS+CDA+CT) with shower array of 1 km^2 in area. **Main physical goals**: the PCR mass composition and energy spectrum in the energy range $E_0 = 10^{14}-10^{18} \text{ эВ}$, hundred TeV γ -astronomy.

A quest of a suitable experimental site



***'Koluch-Kul' experimental site, Eastern Pamirs (37°40'12.68"N,
73°38'52.45"E), H=4250 m a.s.l.***

A quest of a suitable experimental site



'Koluch-Kul' experimental site, Eastern Pamirs, H=4250 m a.s.l.

Tbilisi, 06-07 December 2012

A quest of a suitable experimental site



'Koluch-Kul' experimental site, Eastern Pamirs, H=4250 m a.s.l.

Tbilisi, 06-07 December 2012

Major components and parameters of the *Pamir-XXI* setup

- a deep ($\sim 3,5 \lambda_{\text{int.}}$) lead-carbon **calorimeter** with total area of 192 m² combined with the XREC and burst detector made in the form of solid crosswise lying series of plastic scintillation counters with fiber optic readout (center part);
- two concentric air **shower arrays** around the calorimeter: a dense one with 5 m step of 80 x 80 m² in area and with a high detection threshold, and another more rare array with 85 m spacing of 1 x 1 km² in area and with a low detection threshold;
- a fast timing system (**'chronotron'**) of 8 scintillation points to determine the EAS arrival angles by front arrival delay at different points of the air shower array;
- array of 157 **Čerenkov detectors** spaced throughout the area of $\sim 1 \text{ km}^2$ to determine the shape and the amplitude of the EAS ČL lateral distribution dQ/dR as well as characteristics of the EAS ČL pulse shape, i.e., time distribution dQ/dT and $d^2Q/dRdT$; a step in the central part of the array is 25 m, on the periphery - 85 m (a fast ČD will be either similar to EMI 9350 photomultipliers with a hemispherical photocathode of 20 cm in diameter or will be consist of a 19 PMT matrix placed in the local plane of a mirror of 1.2 m in diameter);
- four wide-angle (with field of view at least 20° and pixel size of PMT mosaic 0,5-1,0°) **Image Čerenkov Telescopes (IACT)** to determine the ČL spatial-angular distribution $d^3Q/dRd\theta_x d\theta_y$ for individual EAS;
- lidar for monitoring the quality of a night atmosphere.

Layout of detectors in *PAMIR-XXI* complex setup

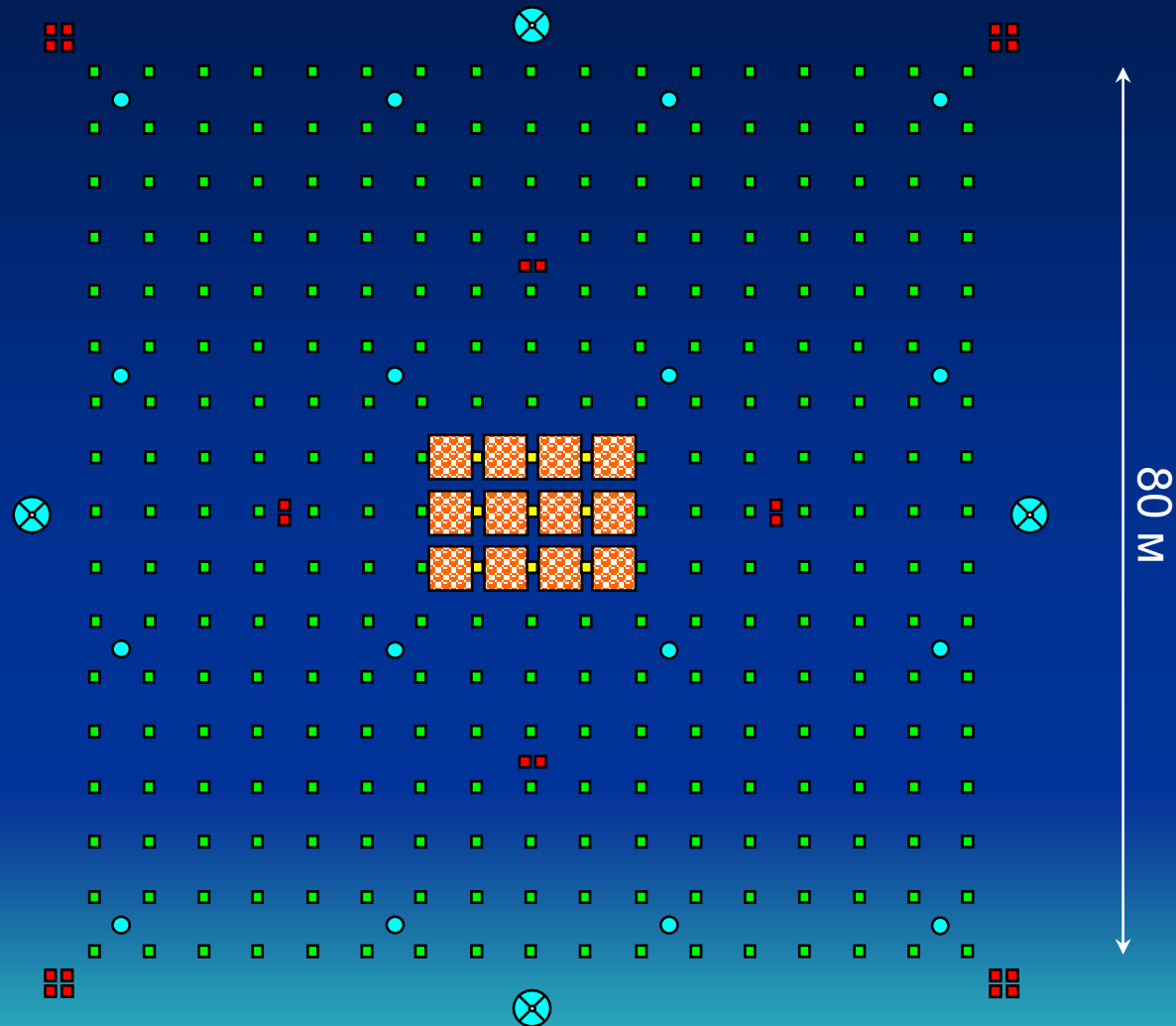
Central part of the shower array.

- - combined detector ($e/\gamma + \mu$) with 0.5 cm Pb at the top, $S = 1 \text{ m}^2$, $N_{\text{c.d.}} = 280$
- - sc-counter (e/γ), $S = 1 \text{ m}^2$, $N = 9$
- - calorimeter section $S = 16 \text{ m}^2$, $N = 12$
- - fast-timing detector ('chronotron' system)
- - Čerenkov light detector
- ⊗ - Image Čerenkov telescope (IACT)

Step – 5 m

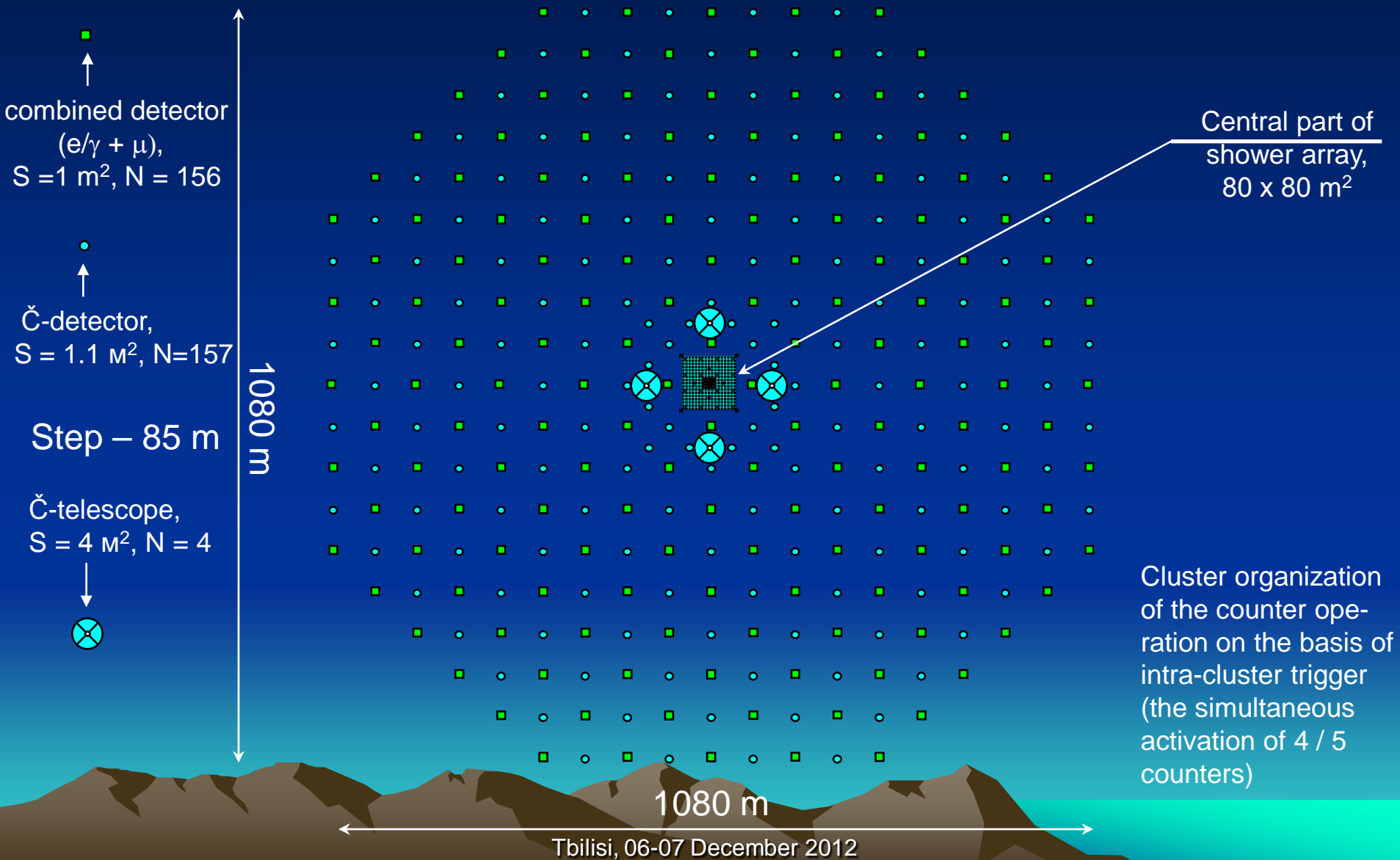


Initial stage: step – 10 m,
 $N_{\text{c.d.}} = 80$

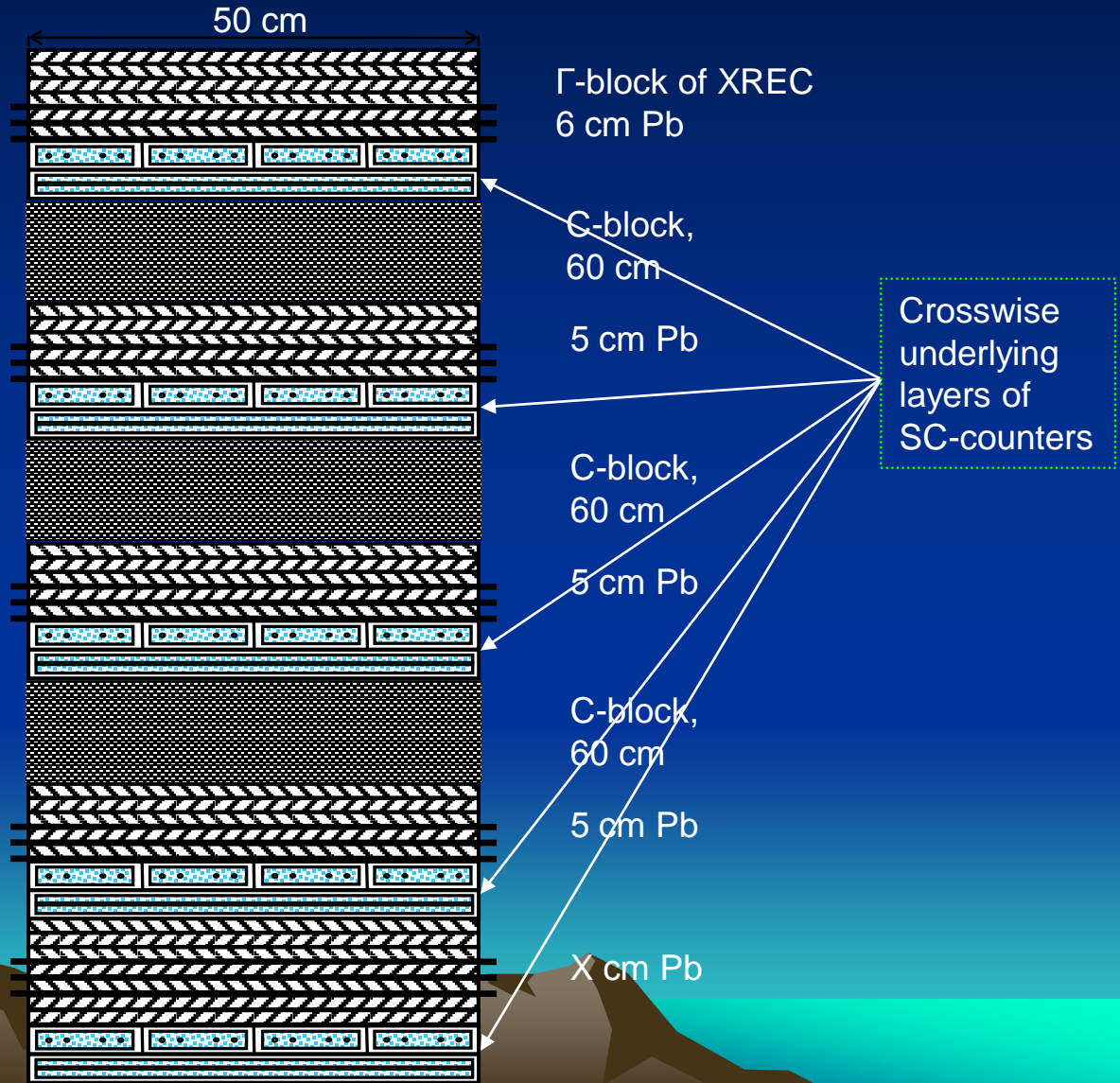


Layout of detectors in *PAMIR-XXI* complex setup

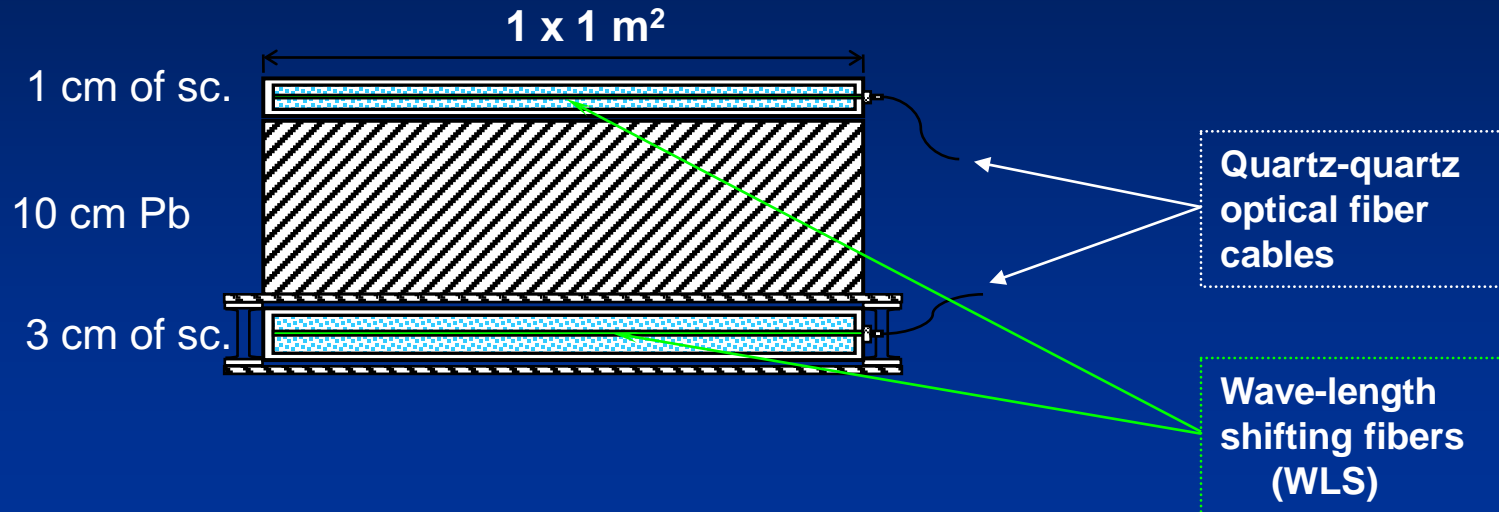
Peripheral part of the shower array.



Design of the hadron calorimeter and the burst detector



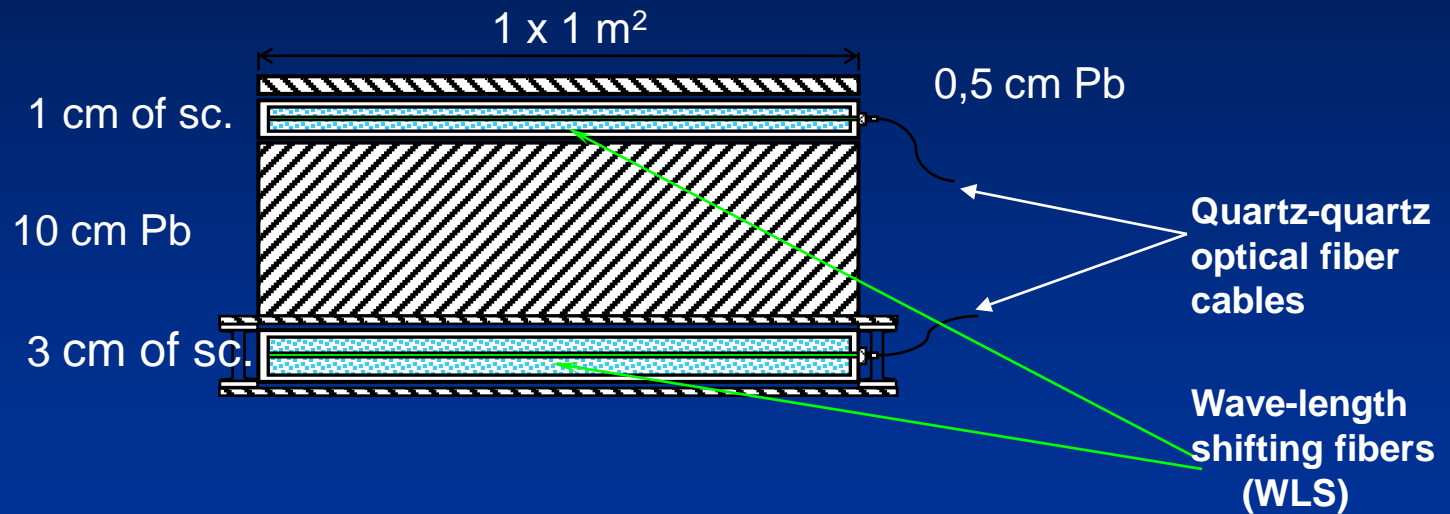
Design of combined $(e/\gamma + \mu)$ detector.



$$E_e^{\text{th}} = 5 \text{ MeV}$$

$$E_\mu^{\text{th}} = 230 \text{ MeV} (H_{\text{Pb}}=10 \text{ cm})$$

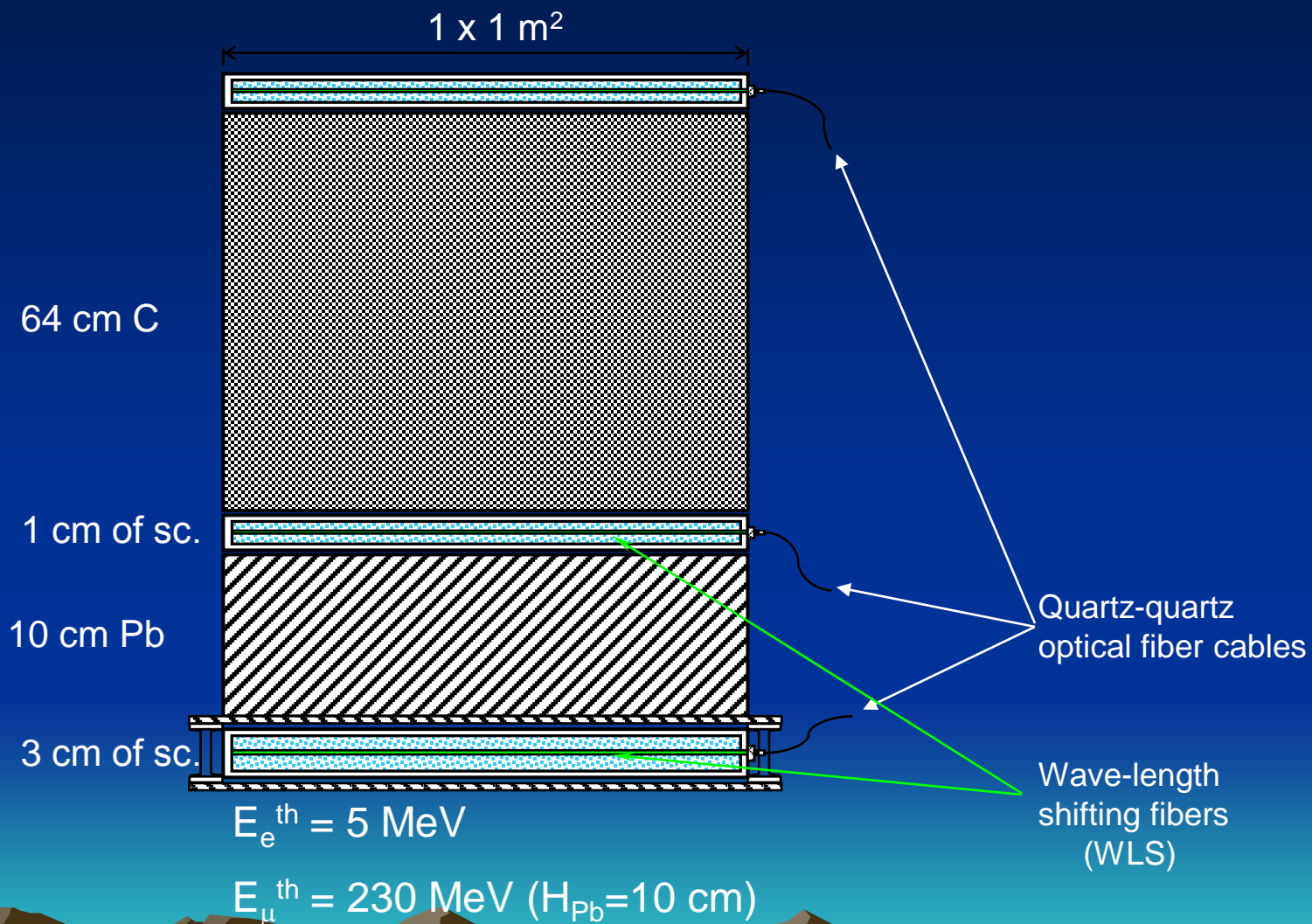
Design of combined $(e/\gamma + \mu)$ detector.



$$E_e^{\text{th}} = 5 \text{ MeV}$$

$$E_\mu^{\text{th}} = 230 \text{ MeV} (H_{\text{Pb}}=10 \text{ cm})$$

Design of combined $(e/\gamma + \mu)$ detector.



Large-stretched plastic scintillation counters with fiber optic readout

The design of combined ($e + \mu$) EAS array detectors as well as burst detectors will use the same type of plastic (polystyrene) scintillation counters of $1 \times 1 \text{ m}^2$ and $0,5 \times 4,0 \text{ m}^2$ in size, respectively, with light collection on the basis of wave-length shifting fibers (WLS) and with fiber optic signal readout that highly increases **uniformity of light collection**.

In this case, the crosswise arrangement of large-stretched scintillation counters used in the burst detector combined with the calorimeter will make it possible to localize EAS core axes with up to **12 cm**. Prototypes of such counters have already been developed and tested at IHEP (Protvino).

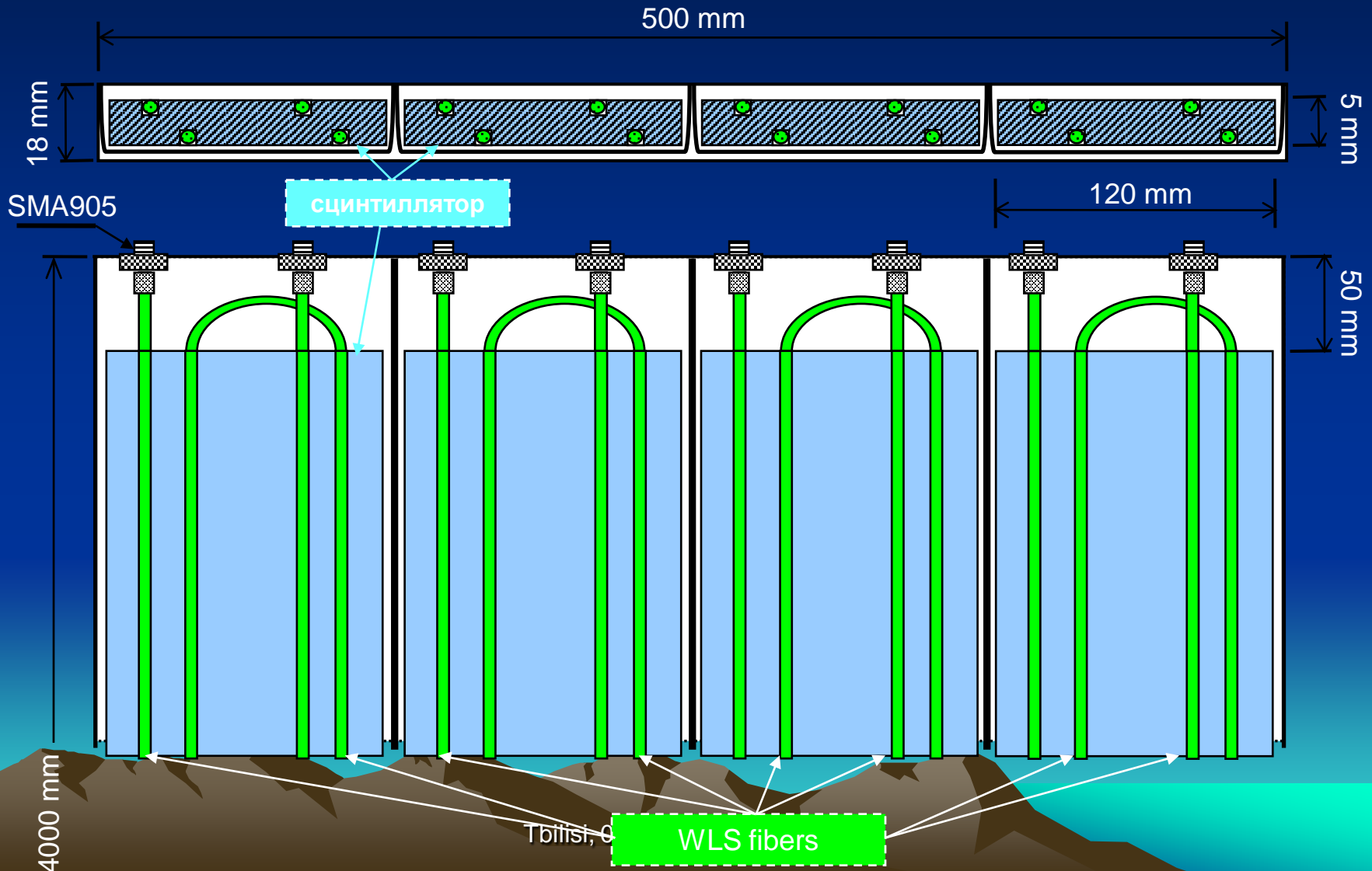
Large-stretched plastic scintillation counters with fiber optic readout

The scintillation counters are manufactured in modules of size 50 x 400 x 1 cm³ hosted in a light-proof duralumin casing.

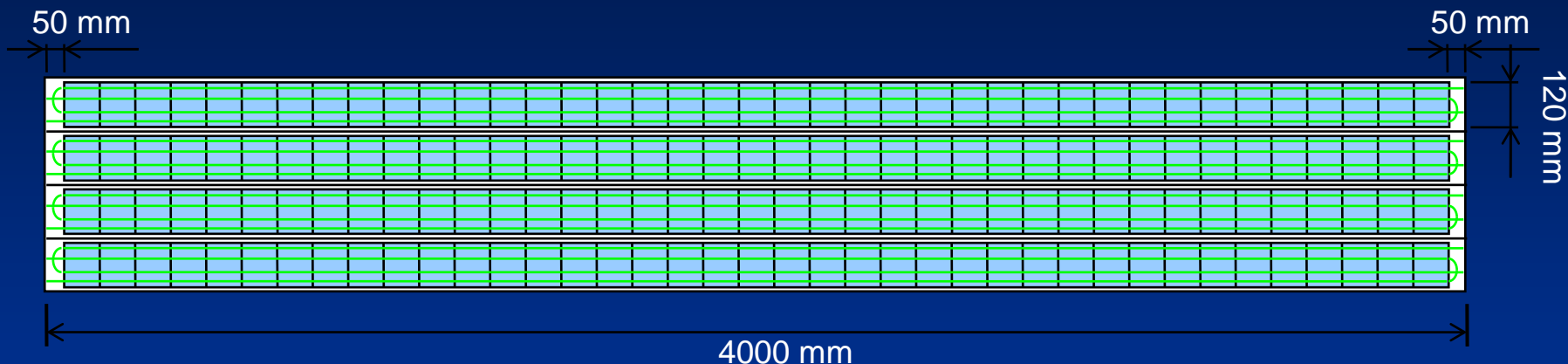
Each module consists of 4 independent strips of scintillator 12 x 390 x 0,5 cm³ in size with four longitudinal grooves into which wave-length shifting fibers (WLS) are embedded which shift the wavelength of light scintillation flash ($\lambda \sim 420$ nm) to an optimum for the photodiode receiver 'green' spectral region ($\lambda \sim 530$ nm) and have low attenuation of the optical signal ($L \geq 3$ m). Reemitting fibers (WLS) are placed with two loops, the ends of each of which are displayed on opposite ends of the module.

In turn, each such strip is assembled from molded polystyrene scintillators of 12 x 10 x 0,5 cm³ with attenuation of the optical signal $\lambda \geq 70$ cm. Each strip in a module is wrapped by light-proof coating with high internal reflectivity (such as Tyvek + Tedlar produced by DUPON).

Design of large-stretched plastic scintillation counters with fiber optic readout



Design of large-stretched plastic scintillation counters with fiber optic readout



Arrangement of scintillation plates of $10 \times 12 \times 0.5 \text{ cm}^3$ in a module

The ends of each fiber loop are sealed in standard opto-mechanical SMA 905 connectors (there are 8 of them at each end of the module in accordance with number of fibers in a strip and number of strips in a module 2×4) for transmission of the light signal to the photo-electronic converter with attached shielded quartz optical fiber.

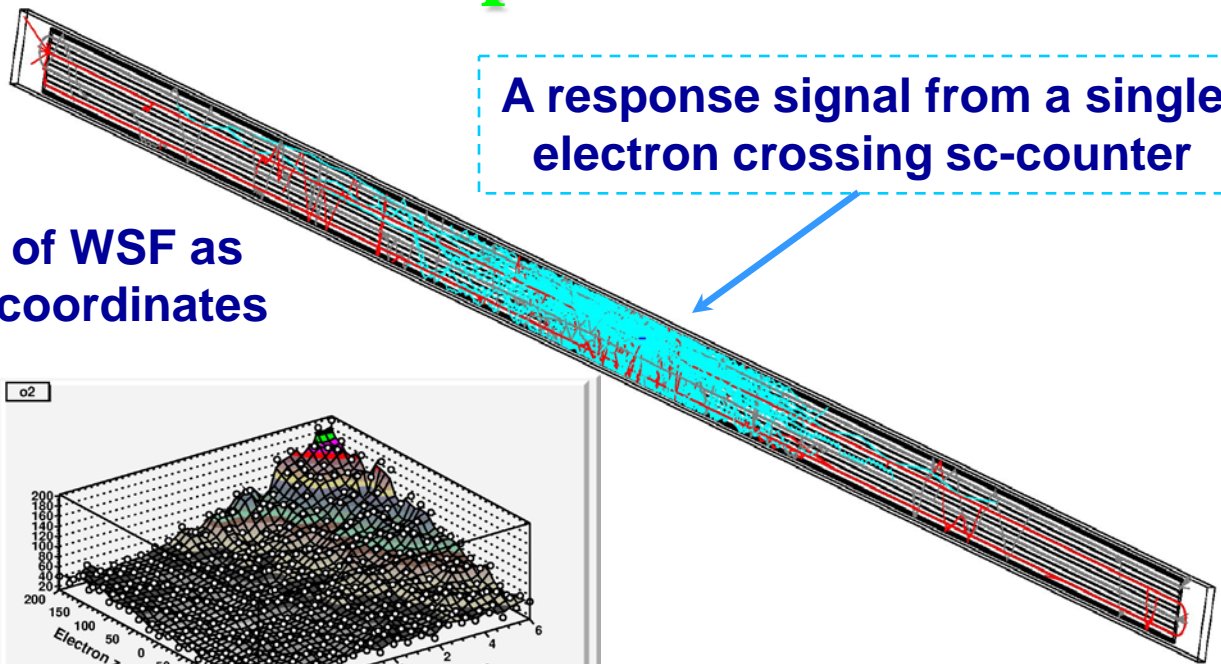
Conversion of optical signals in digital ones will take place in remote thermostatically controlled multichannel low-voltage electronic units based on the modern pin-photodiodes (or silicon photomultipliers) and high-speed (flash) ADC integrated with amplifiers (designer - NPP "Pulsar", Moscow).

Production of large-stretched plastic scintillation counters with fiber optic readout



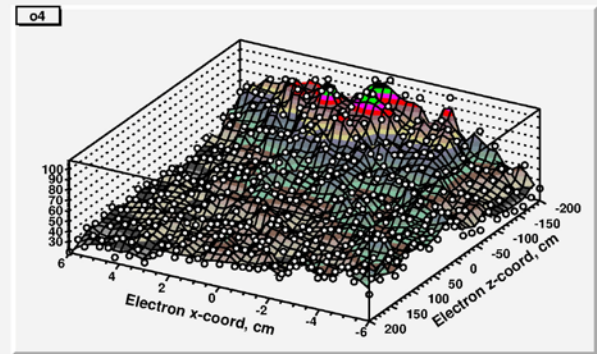
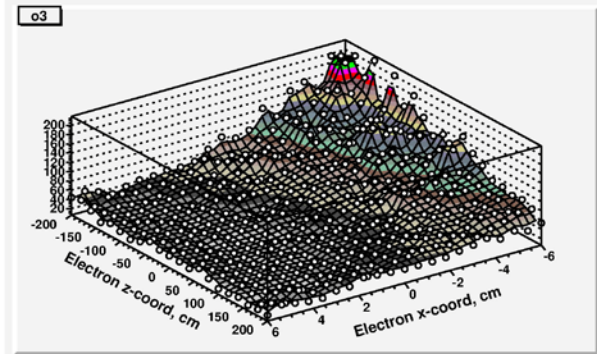
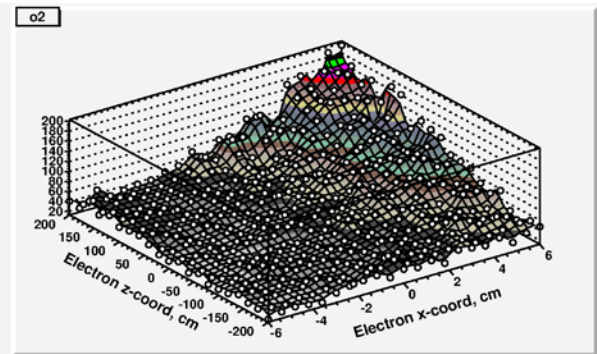
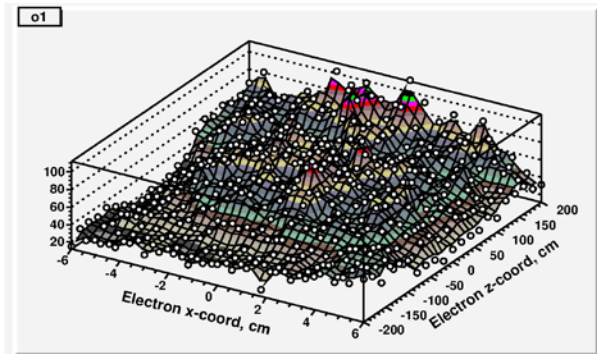
Tbilisi, 06-07 December 2012

Simulation of the hybrid calorimeter/large-stretched plastic scintillation counter response with GEANT4.9.4.p02

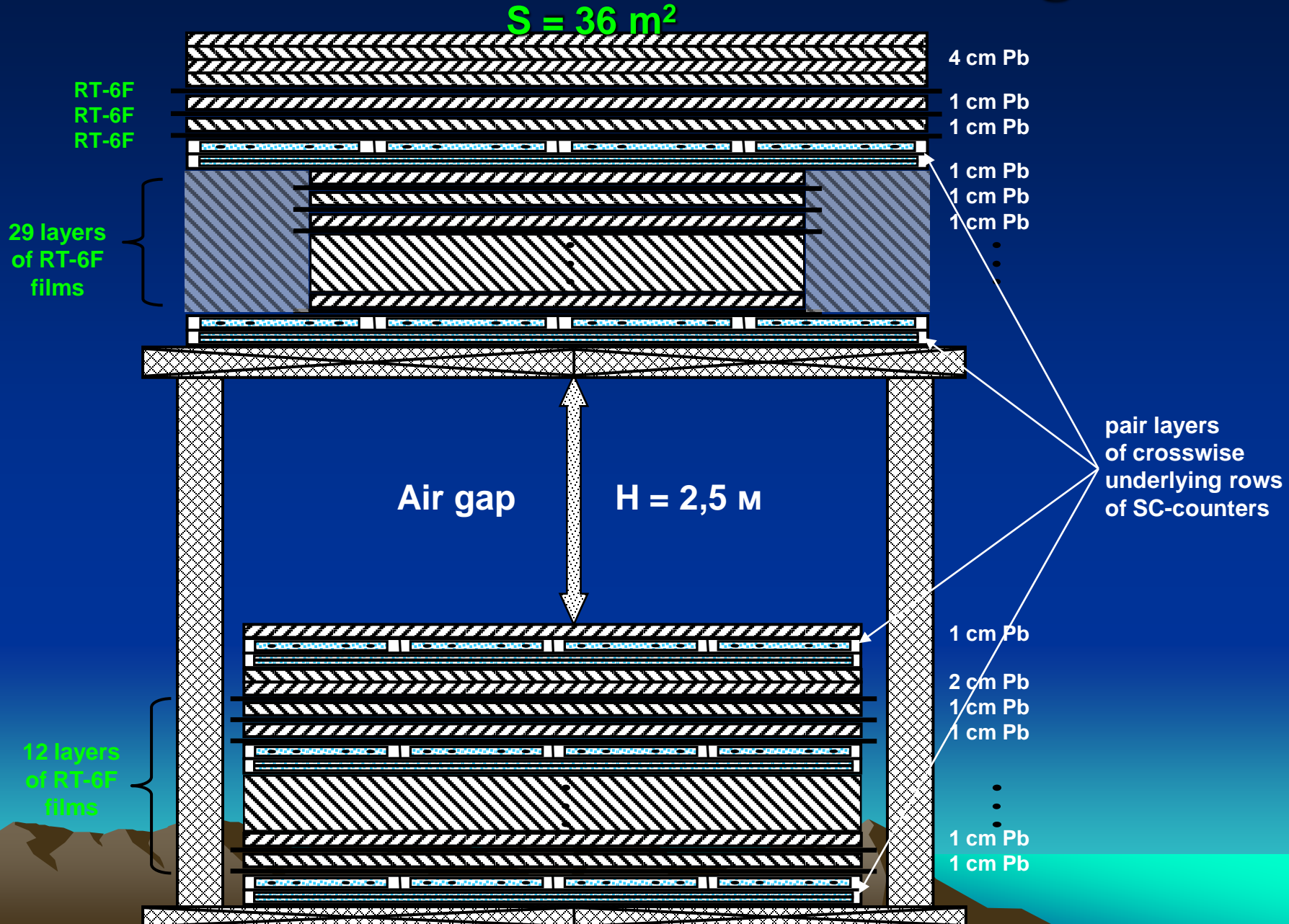


A response signal from a single electron crossing sc-counter

Light signals at the 4 ends of WSF as a function of the entrance coordinates



Search for 'Centaurus' and strangelets

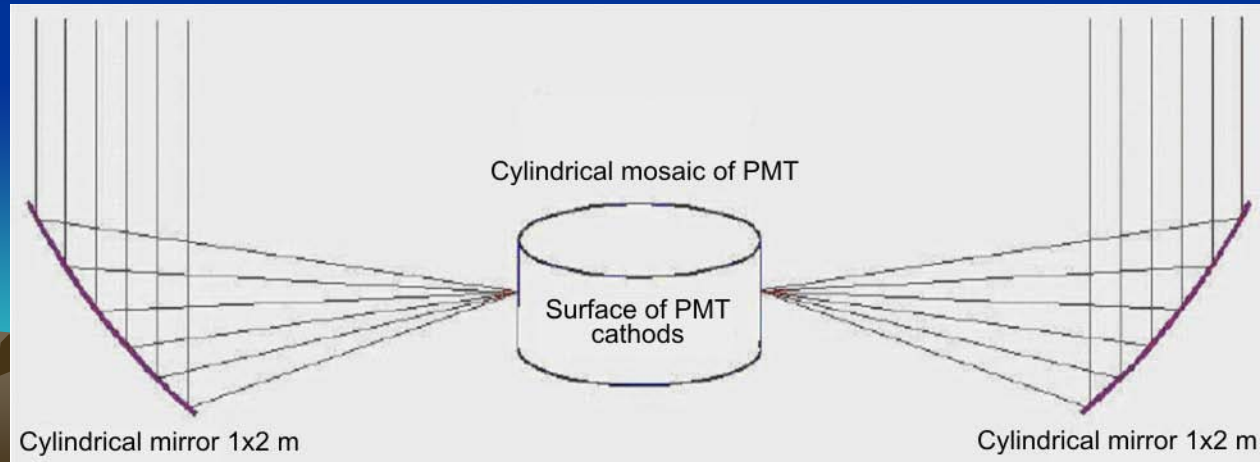
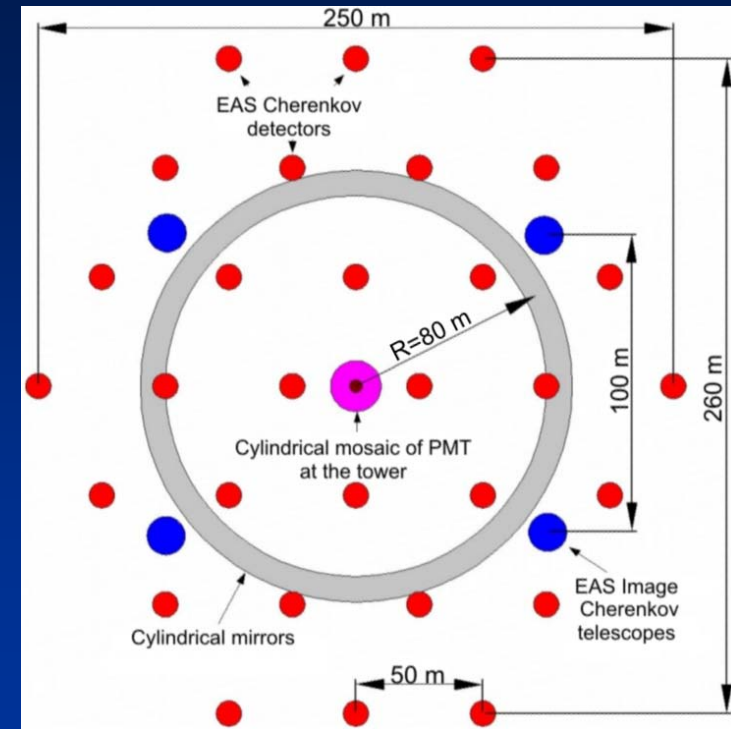
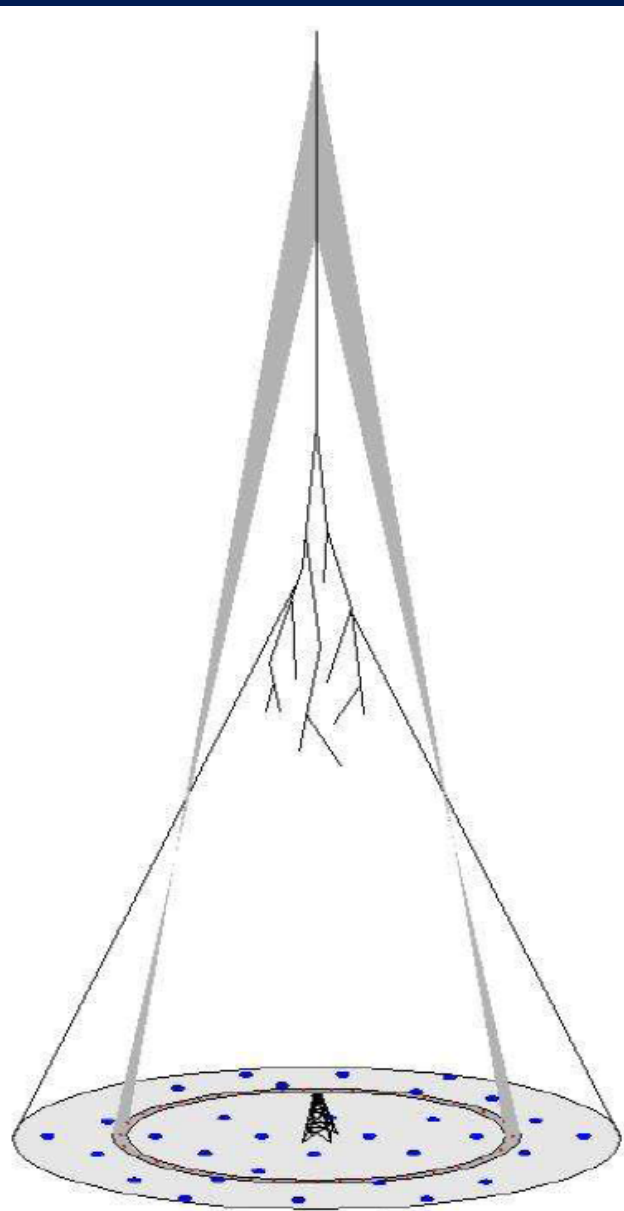


Detection of direct Čerenkov emission

(project by R.A.Antonov, D.V.Chernov, etc. – SINP MSU)

Combined Čerenkov setup:
 $(E_0 = 10^{14} \div 10^{16} \text{ эВ})$

- $E_0, (\theta, \varphi), (x_0, y_0)$
- $Z_0 (Q \sim Z^2)$
- A_0



Detection of direct Čerenkov emission

(project by R.A.Antonov, D.V.Chernov, etc. – SINP MSU)

EAS Cherenkov detectors:

- mirror diameter: 1-1,2 m
- number of PMT in a mosaic: 19
- field of view: 25°
- counting frequency of impulse shape for each PMT: 2 ns
- dynamic range: 10^5
- angular positioning system: $180^\circ \times 360^\circ$
- accuracy of light yeild calibration with lasers for all detectors over all angles : $< 5\%$

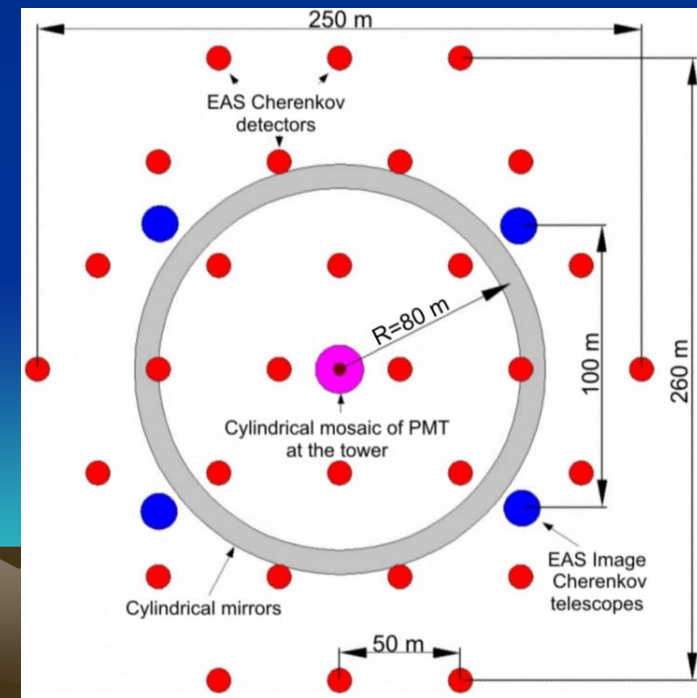


Angular resolution of EAS axis determining $\sim 0,05^\circ$

Spatial resolution of axis coordinate determining ~ 1 m

EAS Image Cherenkov telescopes:

- mirror diameter: 3-4 m
- number of PMT in a mosaic: 1250
- field of view: 20°
- angular resolution: $0,5^\circ$
- counting frequency of impulse shape for each PMT: 2 ns (5 ns)
- angular positioning system: $180^\circ \times 360^\circ$



PAMIR-XXI setup

capabilities for physical measurements

- on event-determination of the energy flux lateral distribution (LDF) for electron-photon, hadron and muon EAS components, as well as for that of Čerenkov radiation;
- measuring coordinates and energy of the most energetic particles in the EAS core with XREC data;
- measuring stellar coordinates of EAS arrival;
- calorimetric determination of the primary particle energy E_0 by measuring the energy of each EAS component;
- separation of events for the main groups of nuclei;
- selection of EAS from the primary γ -rays;
- determination of the primary particle energy E_0 with an accuracy of $\sim 15\%$ and maximum EAS development depth X_{\max} with an accuracy of $\sim 30 \text{ g/cm}^2$ with EAS ČL for individual showers;
- determination of the primary particle charge by the direct Čerenkov radiation;

PAMIR-XXI setup

capabilities for physical measurements

- determination of the mass composition of the PCR for the main groups of nuclei with the average atomic numbers: $A = 1, 4, 14, 26, 56$ in the 'knee' and above;
- receiving elementwise (partial) spectra of PCR in a wide energy range $E_0 = 0.03 \div 1000 \text{ ПэВ}$ and determination of 'fine' structure of the 1-st break the spectrum in the $1 \div 100 \text{ PeV}$ region using various EAS components and different but mutually calibrated techniques;
- carrying out of exclusive measurements in order to study correlation characteristics of the main EAS components;
- detailed study of the EAS core structure;
- study of semi-inclusive spectra of secondary hadrons based on the knowledge of primary particle energy E_0 with good accuracy;

PAMIR-XXI setup

capabilities for physical measurements

- refinement of characteristics of multiple particle production in the forward (fragmentation) kinematic region and parameters of nuclear interaction models at energies up to $E_0 \leq 10^{18}$ eV, taking into account the complementary character of collider data and those of CR experiments;
- selection, from the total EAS flux, showers with anomalies as according to the XREC data and with respect to spatial, energy and temporal characteristics of the main EAS components in order to study their mutual correlations;
- study of new (exotic) phenomena, i.e., the coplanar emission of particles in multiple production at very high energies, the events with an abnormal ratio of charged to neutral hadrons (the Centauro-type events), generation of high- p_t 'halo' events, abnormal absorption of nuclear-active penetrating CR particles ('long-flying' component, strangelets, etc. ?);

PAMIR-XXI setup

capabilities for physical measurements

- identifying the nature of the primary particles, generating abnormal events, determining the main characteristics of their interaction in atmosphere and understanding of their possible influence on the formation of the PCR energy spectrum;
- reality check of the second break in the PCR energy spectrum at energies ~ 100 PeV, determining of its parameters to identify its nature;
- direct measurements of nuclear interaction characteristics at energies up to $E_0 \leq 10^{18}$ eV by selecting events with only one interaction over the setup, as well as detection of skipped protons to determine the p-air inelastic cross sections;
- receiving of the energy spectrum of the diffuse γ -radiation at energies 30 - 2000 TeV using the method of hadron-less and muon-less air shower registration, as well as obtaining distribution of their arrival coordinates on the celestial sphere;

PAMIR-XXI setup

capabilities for physical measurements

- detailed study of a broad range of the PCR spectrum ($E_0=30\div 10^6$ TэВ) for each nucleus species will provide an important link between direct measurements on balloons and spacecrafts with the results of UHECR experiments and will make it possible to fix characteristics and to perceive the nature of the transition from galactic cosmic rays to extragalactic ones with localizing the relevant boundary region.

PAMIR-XXI setup

capabilities for advance of technique

- cross check of different techniques of the PCR energy E_0 and mass A recovery by the observed characteristics of different EAS components;
- calibration of EAS techniques with direct measurement data

Welcome to the Pamirs!

